

Cite as: G.M. Verderame, F. De Luca, M.T. De Risi, C. Del Gaudio, P. Ricci (2012), *A three level vulnerability approach for damage assessment of infilled RC buildings: The Emilia 2012 case (V 1.0)*, available at <http://www.reluis.it>.



A THREE LEVEL VULNERABILITY APPROACH FOR THE DAMAGE ASSESSMENT OF INFILLED RC BUILDINGS: THE EMILIA 2012 CASE (v 1.0)



Gerardo Mario Verderame, Flavia De Luca, Maria Teresa De Risi, Carlo Del Gaudio, Paolo Ricci
gerardomario.verderame@unina.it, flavia.deluca@unina.it, mariateresa.derisi@unina.it, carlo.delgaudio@unina.it,
paolo.ricci@unina.it

Dipartimento di Ingegneria Strutturale, Università degli Studi di Napoli Federico II.

Index

1	Introduction	2
2	Emilia building stock and classification.....	3
2.1	Official statistical data on the building stock	3
2.2	Evolution of the seismic classification in the Emilia region	5
2.3	Benchmark structures	7
3	Vulnerability approaches and earthquake damage assessment.....	9
4	EXACT vulnerability approach.....	12
4.1	Simulated design procedure	12
4.2	Numerical model	12
4.3	Analysis methodology	14
4.4	Results	17
5	POST vulnerability approach.....	19
5.1	Input data.....	20
5.2	Simulated design procedure	21
5.3	Characterization of nonlinear response	22
5.4	Seismic assessment.....	23
6	FAST vulnerability approach	28
6.1	Simplified simulated design procedure	29
6.2	Evaluation of the approximate capacity curve of RC infilled building.....	30
6.3	Seismic assessment.....	33
7	Comparative damage assessment	38
8	Conclusions and Perspectives.....	45

1 INTRODUCTION

On the 20th of May the Emilia region was struck by a magnitude (M_w) 6.0 (according to USGS) earthquake. The highest PGA registered at the closest station from the epicenter was equal to 0.27g approximately (Chioccarelli et al, 2012a). The event involved a large area between the provinces of Modena, Ferrara, Rovigo and Mantova. Main damage involved historical buildings, masonry buildings, industrial structures, and in some cases also reinforced concrete structures, as shown by in-filed reports after the earthquake (e.g., EPICentre Field Observation Report No. EPI-FO-200512, 2012; EPICentre Field Observation Report No. EPI-FO-290512, 2012; Decanini et al., 2012). The mainshock was followed by a M_w 5.8 (according to INGV) aftershock on the 29th of May (Chioccarelli et al., 2012b) and the whole seismic sequence from the 16th of May up to the 26th of June was characterized by seven events with magnitude equal or higher than 5.0 (<http://www.ingv.it/it/>).

Notwithstanding the fact that a single event cannot be employed to validate hazard data adopted by codes for design and assessment (Iervolino, 2012), a comparison with ground motion prediction equations and code spectra for the area can still be done (Iervolino et al, 2012). The preliminary comparison with elastic and inelastic ground motion prediction equations (Bindi et al., 2011; De Luca, 2011), and code spectra (DM 14/01/2008) provided right after the event (Chioccarelli et al, 2012a), showed that earthquake magnitude and location are consistent with the ranges considered by the Italian national hazard data (i.e., Stucchi et al., 2011), and ground motion values are in general agreement with prediction equation and code spectra.

According to the latter remarks, the observed damage after the event seems to be in some way “unexpected”, especially if referred to reinforced concrete structures. On the other hand, looking into the evolution of the seismic classification of the area, and crossing such information with the characteristics of building stock, it can be observed that most representative reinforced concrete buildings are designed for gravity loads and seldom have more than four storeys, (see section 2).

The general characteristics of the building stock and the seismic evolution of the code classifications allow the definition of three benchmark buildings that can be considered as representative structures for the application of an EMS-98 based (Grunthal, 1998) damage assessment, developed at three different level, and based on infill damage state only, (see section 3).

The working hypotheses and damage assessment results for each level of vulnerability approach applied to the Emilia region are provided in section 4, 5, and 6, respectively. First of all a detailed static pushover based vulnerability approach is pursued (see section 4), in the following referred as

EXACT, (Ricci et al, 2012). Secondly the results obtained on the three benchmark buildings are provided through a mechanical based vulnerability approach, suitable for large scale assessment (see section 5), also known as *POST* (Ricci, 2010). Finally, damage assessment results based on an empirical-mechanical approximated approach are shown (Gomez-Martinez et al., 2012, De Luca et al. 2012), referred in the following as *FAST*, (see section 6). The latter can be suitable for rapid large-scale assessment or for emergency management right after seismic events (e.g., Goretti and Di Pasquale, 2006).

A comparison of the results of the three vulnerability approaches is shown in section 7, and finally crossed with the Peak Ground Acceleration (PGA) shake map provided by INGV right after the earthquake (<http://www.ingv.it/it/>).

2 EMILIA BUILDING STOCK AND CLASSIFICATION

The definition of the benchmark structures for the three level vulnerability approach is made through a two step process. The first step is to analyze the official data in terms of number of storeys and age of construction for the area struck by the earthquake. The second step is pursued looking into the evolution of the seismic classification of the area. **Official statistical data on the building stock**

Emilia–Romagna is one of the richest, most developed regions in Europe, and it has the third highest “gross domestic product” per capita in Italy. Bologna, its principal city, has one of Italy's highest quality of life indices and advanced social services. Indeed, almost 5% of the whole building stock is constituted by buildings or group of buildings used as hotels, offices, commerce and industry, communications and transport (Figure 1a), according to Istat data.

The Istat (Italian National Institute of Statistics) survey is a nation-wide census that provides information on citizens, foreign, buildings and dwellings. In particular, in the “14th general census of the population and dwellings” (*14° Censimento generale della popolazione e delle abitazioni, ISTAT 2001*) information about the number of storeys, as well as characteristic of residential buildings, and in some cases even those non residential, are provided.

For instance, the availability of such data allows to carry out the statistics of buildings in terms of number of storeys (one-, two-, three-storeys and four or more storeys buildings), age of construction (typically with a decennial-rate) and building typologies (masonry or reinforced concrete buildings) for the spatial unit, the so called *cell*. Nevertheless, due to confidentiality requirements, these statistics were presented in an aggregate manner, in which the information is not immediately recognizable as a function of the identified classes; for example, it is not possible

to get the number of reinforced concrete (RC) buildings in a cell, date back to a specific age of construction and characterized by a given number of storeys. In the following the statistics for the 448 Municipality hit by the 2012 earthquake are shown, see Figure 1.

Among the whole building stock of the area struck by the earthquake only 20% is constituted by RC (Figure 1b). Almost 75% of the buildings is characterized by a number of stories lower or equal than two (Figure 1c). Regarding this latter aspect, it should be noted that the number of storeys is referred to all the buildings and it can be inferred that among the 60% of the two storeys buildings the main part is masonry. A uniform rate over the years with respect to the age of construction of the buildings can be observed from data shown in Figure 1d. Data from Figure 1 allow to infer that the RC building stock is characterized mostly by low to medium rise buildings (from to 2, up to 4 storeys) and almost 60% of them was realized between 1960 and 1980.

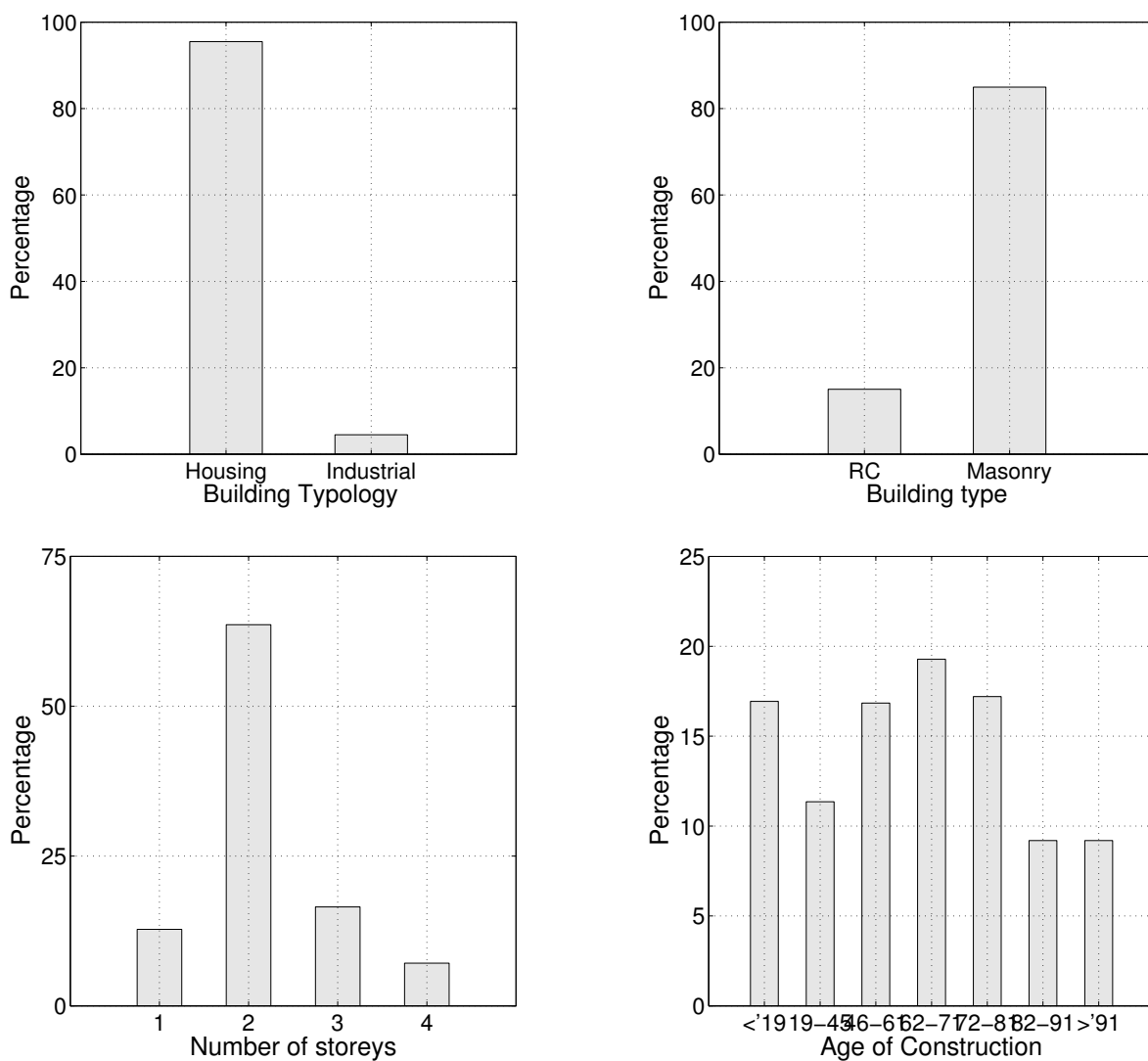


Figure 1. Statistics for the 448 Municipality hit by the earthquake of 20th of May 2012: percentages with respect to building typology (a), building type (b), number of storeys (c), age of construction (d).

2.2 Evolution of the seismic classification in the Emilia region

Seismic classification in Italy and in general in all seismically prone areas is quite often a result of disastrous earthquakes. In Italy, the first classification was released in 1909 after the disastrous earthquake of Reggio Calabria and Messina in 1908. Obviously such a classification was updated at the knowledge of the time. After this first classification every five or ten years a new update of seismic classification and code provisions were provided (Lai et al., 2009).

In recent years, four are the fundamental dates for the evolution of the seismic classification in Italy: 1984, 1998, 2003, and 2008. In fact, after the Friuli (1976) and Irpinia (1980) disastrous earthquakes, three different seismic categories were classified, and the third category, characterized by a PGA equal to 0.04g, was firstly introduced. First and second categories were characterized by a PGA equal to 0.10g and 0.06g, respectively (Ricci et al., 2011a). Such accelerations were determined through the seismic coefficient S equal to 12, 9, and 6, and decreasing with the increasing of the category from first to third. According to the latter classification (De Marco and Marsan, 1986) most of the area struck by the 2012 Emilia earthquake was classified as non seismic (Figure 2a).

Successively, in 1998, a reclassification proposal was provided by the Servizio Sismico Nazionale. Such a classification was never adopted officially by any code but it is at the basis of the classification made in 2003 (OPCM 3274, 2003) after the San Giuliano earthquake. The 2003 regulation document introduced also modern design rule such as the so called capacity design. On the other hand, it should be noted that such rules worked as recommendation, since they have never become compulsory, and it was still possible to design new structures according to the previous building code (DM 16/01/1996).

According to 1998 classification the area struck by the 2012 earthquake was firstly classified as seismic, in the so called third category (0.04g). Successively, in the classification of the OPCM 3274, the whole area was still in third category; on the other hand a design PGA of 0.15g on rigid soil was employed; being the PGA with 10% probability of exceedance in 50 years of such areas comprised in the range 0.05-0.15g.

The 2003 classification and the design provisions (OPCM 3274, 2003), even if they were not compulsory, represented the “Copernican revolution” of Italian earthquake engineering, since it was the first step towards the European unified design approach provided by Eurocodes and the first introduction of modern seismic design rules. In particular, the OPCM 3274 (2003) was very similar to the provisions provided in Eurocode 8 or EC8 (CEN, 2004).

The last step in terms of seismic classification was made in 2008, when the [DM 14/01/2008](#) was released. In the 2008 code the seismic input is based on specific hazard data based on a 5km spaced grid ([Stucchi et al., 2011](#)) and spectral shape is site dependant, ending up in a code spectra very close to a uniform hazard spectrum (UHS) PGA on rigid soil according to 2008 code are shown in as shown in [Figure 2b](#).

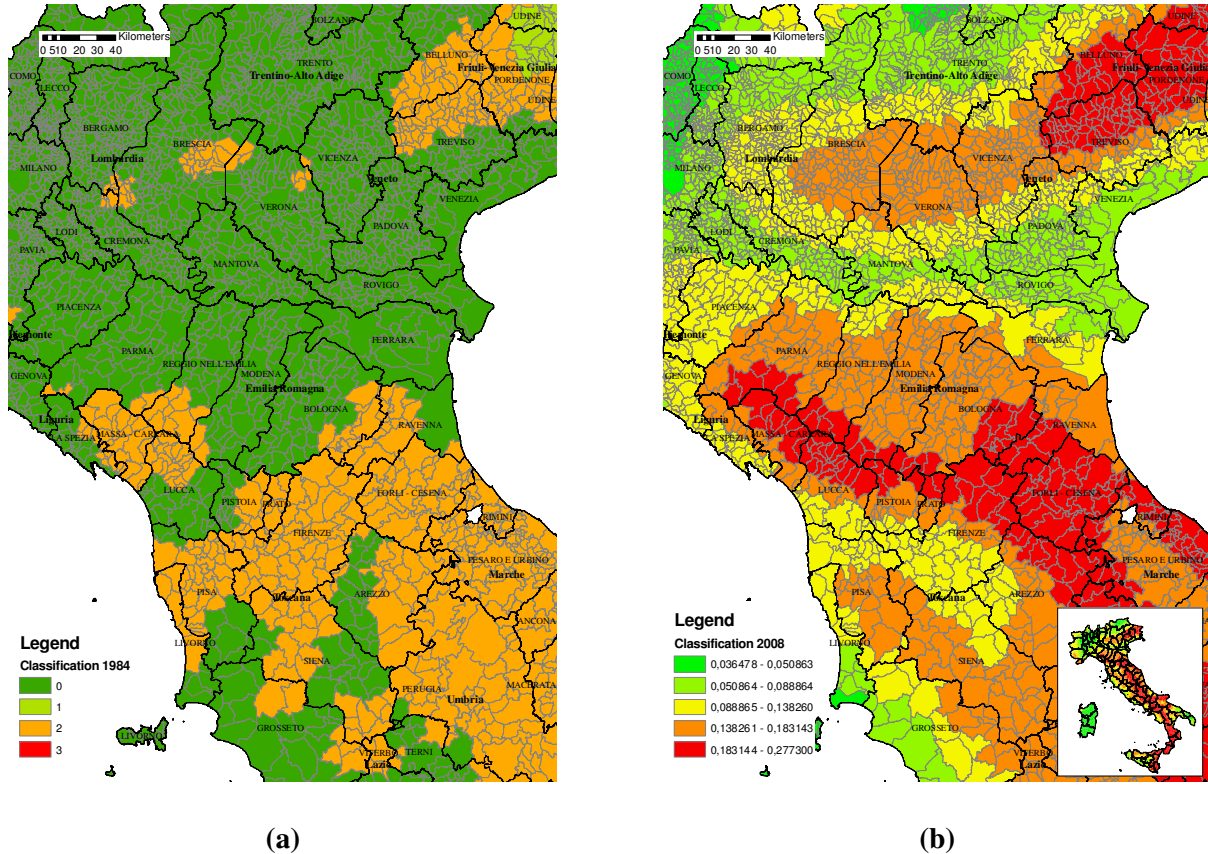
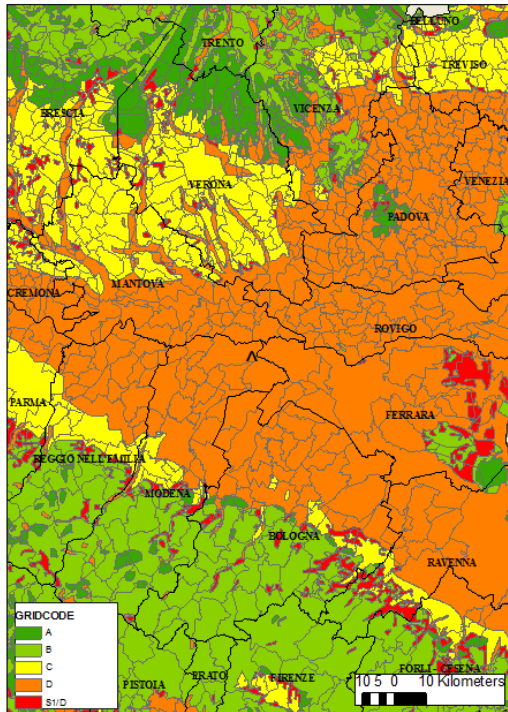


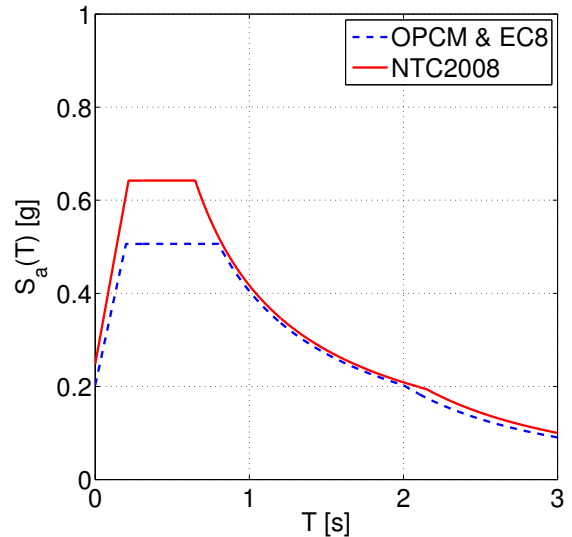
Figure 2. Seismic classification before 1998, according to De Marco and Marsan (1986), (a); and actual classification according to the official hazard data ([Stucchi et al, 2011](#)) employed in [DM 14/01/2008](#), (b).

In [Figure 3](#) the geological classification of the soil according to EC8 and the code spectra according to OPCM 3274, EC8 and DM 14/01/2008 are evaluated for the epicenter of the event of the 20th of May. The only spectra according to actual Italian seismic code ([DM 14/01/2008](#)) is dependent on the geographic coordinates and spectral shape depends on the probability of exceedance considered (in this case 10% in 50 years), while both OPCM 3274 and EC8 spectra depends on the seismic zone and soil class only. The value of PGA on rigid soil is equal to 0.138g according to DM 14/01/2008, while it is equal to 0.15g in the case of OPCM and EC8. On the other hand, the soil amplification factor for D soil type is 1.8 in the case of the Italian code and 1.35 in the case of EC8 (type 1) and OPCM. Soil D was chosen for this code spectral comparison because it is the most frequent class in the whole epicentral area. In the following all spectral based approaches

are going to be pursued considering the EC8 spectra in [Figure 3b](#). Given the fact they are similar, it is preferable to consider a single spectra that in some way accounts for the general characteristics of the vast area struck by the earthquake.



(a)



(b)

Figure 3. Soil classification on geological basis of the area struck by the earthquake (a); comparison of code spectra according to EC8, OPCM 3274, and DM14/01/2008 for D soil class at the epicenter of the event of the 20th of May (lat. 44.89, long. 11.23), (b).

It should be finally noted that the 2008 code became the official Italian code and the only one to be employed only in July 2009, after the 2009 L'Aquila earthquake.

According to the previous observations, and considering that most of the building stock was realized between sixties and eighties it is easy to recognize that most of the area struck by the 2012 Emilia earthquake was designed for gravity loads. Another support reason for the choice of gravity load designed structures as representative of the whole RC building stock of the area is that in the case of mid rise RC buildings and medium-low seismicity design the gravity loads still rule the design, as long as capacity design is not employed (e.g., [Benavent-Climent, 2004](#)).

2.3 Benchmark structures

Data and information in the previous section allow the definition of the benchmark structures employed in this study. The structures analyzed are symmetric in plan, both in longitudinal (X) and

in transverse (Y) direction, with five bays in longitudinal direction and three bays in transverse direction. Interstorey height is equal to 3.0 m, bay length is equal to 4.5 m. Hence, the global plan extension is equal to (22.5x13.5) m². Slab way is always parallel to the transverse direction.

Two-, four- and six-storey buildings are considered - according to the typical number of storeys characterizing Emilia's RC building stock - with the same plan distribution of beams, columns and infill panels. Infills panels are uniformly distributed in all of the external frames; their thickness is equal to 20 cm and presence of openings is not taken into account. The geometric percentage of infilled area respect to the global plan extension (ρ_w) is equal to 0.028 and 0.017 in longitudinal and transverse direction, respectively. Dead load is equal to 5.00 kN/m² and live load is equal to 2 kN/m². Mechanical properties for RC elements and infill panels are reported in Table 1.

The three structures defined, even if characterized by specific geometric and mechanical properties can be considered as representative of RC residential building stock, given the previous observations on the building stock and seismic classification. Once their characteristics are defined, the three vulnerability approaches considered, and presented in the following, can be applied in a comparative framework between each other and with respect to the registered acceleration of the Emilia 2012 event.

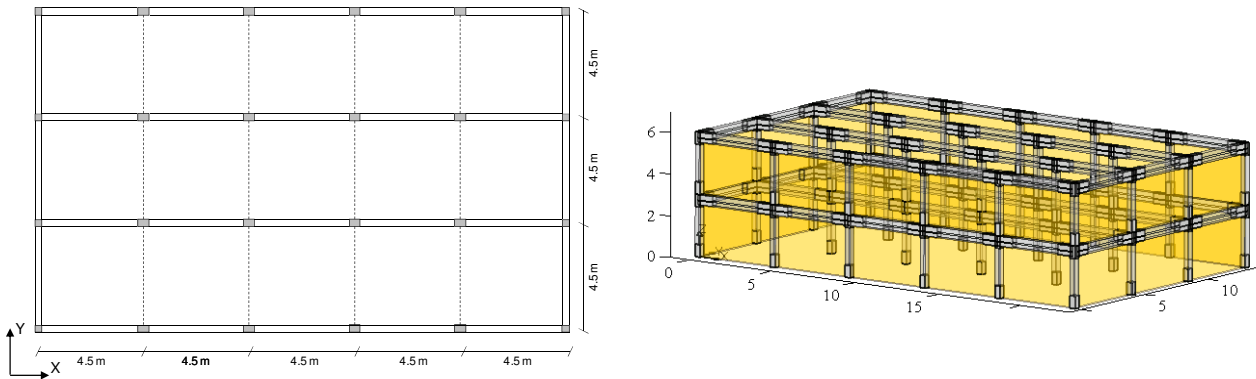


Figure 4. Plan view of case study buildings and 3D view of the 2-storey building

Table 1. RC and infill mechanical properties

	Mechanical property	Value
RC	Concrete compressive strength, f_c	25.0 MPa
	Steel yield strength, f_y	369.7 MPa
Infill	Shear elastic modulus, G_w	1240 MPa
	Young elastic modulus, E_w	4133 MPa
	Shear cracking stress, τ_{cr}	0.33 MPa
	Softening-to-elastic stiffness ratio, α	3%
	Residual-to-maximum stress ratio, β	1%

3 VULNERABILITY APPROACHES AND EARTHQUAKE DAMAGE ASSESSMENT

Vulnerability represents with the so called exposure the part of seismic risk in which engineers, practitioners, and governments can play a crucial role. The first depends on the main characteristics of the building stock, and the design rules according to which such building stock was realized. The study and the interpretation of structural behaviour become crucial in prevention, mitigation, and after earthquake management. Each of the latter actions ask for different level of detailing and accuracy in the approach.

The main framework of vulnerability approaches can be divided in three main groups: (i) approaches that select a representative building of the building stock to be studied and consider only the intra-building variability (e.g., [Rossetto and Enlnashai, 2005](#)); (ii) approaches that analyze building classes considering directly both intra- and inter-building variability so introducing uncertainties within the class of structures (e.g., [Cosenza et al, 2005](#); [Iervolino et al., 2007](#); [Ricci, 2010](#)); (iii) approaches based on both mechanical and empirical basis that define approximately the capacity curve (e.g., [Giovinazzi and Lagomarino, 2004](#); [Giovinazzi, 2005](#)).

The two approximate approaches for large scale assessment provided herein can be respectively collocated in the second and third group; in fact the *POST* continues, by means of the introduction of structural infill contribution, the ideal outline of building classes vulnerability approaches; while the *FAST* provides a rapid assessment on a hybrid mechanical- empirical basis and it is ideally close to the third group of approaches.

All the vulnerability approaches end up in a comparison with observed damage data collected after earthquakes. The collection of damage data asks for an objective classification of the damage for each building type. In this framework the macro seismic intensity scale plays a significant role.

Macro seismic intensity scales classify the severity of an earthquake by means of damages induced on civil structures and on territory. The most utilized in Europe are the Mercalli Scale, dating at the beginning of '900, which through a series of modification and improvement gave rise to the Mercalli-Cancani-Sieberg Scale, and the European Macroseismic Scale (EMS).


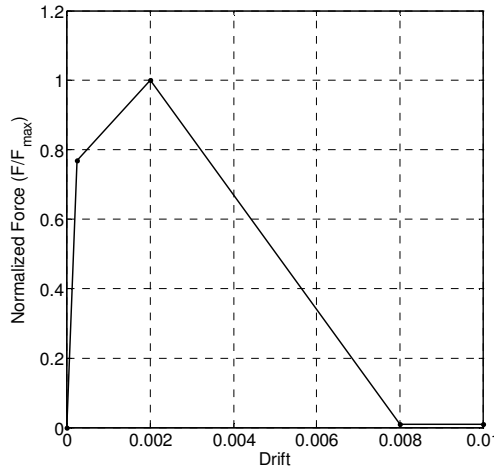


EMS is the basis for evaluation of seismic intensity in European countries and it is also used in a number of countries outside Europe. Issued in 1998 as an update of the test version from 1992, the scale is referred to as EMS-98 ([Grunthal, 1998](#)). A different classification of damage is provided for masonry and infilled RC structures.

The EMS-98 scale involves five grades of damage (in the following they are referred as DS_i) from *slight* damage up to *destruction*, passing through *moderate*, *heavy* and *very heavy* damage. For each level an increasing characterization of damage to masonry infills (nonstructural elements) and

RC elements (structural elements) is provided, each single DS is characterized by a classification of both structural and non-structural damage.

In second column of [Table 2](#) is reported the classification of the first three DS for RC buildings described in EMS-98 and the mechanical interpretation relative to displacement thresholds in secondary elements.

Table 2. RC and infill mechanical properties

	<p>Grade 1: Negligible to slight damage (no structural damage, slight non-structural damage)</p> <p>Fine cracks in plaster over frame members or in walls at the base. Fine cracks in partitions and infills.</p>	<p>DS 1:</p> <p>Δ_{cr}^{inf}</p>	
	<p>Grade 2: Moderate damage (slight structural damage, moderate non-structural damage)</p> <p>Cracks in columns and beams of frames and in structural walls. Cracks in partition and infill walls; fall of brittle cladding and plaster. Falling mortar from the joints of wall panels.</p>	<p>DS 2:</p> <p>Δ_{max}^{inf}</p>	
	<p>Grade 3: Substantial to heavy damage (moderate structural damage, heavy non-structural damage)</p> <p>Cracks in columns and beam column joints of frames at the base and at joints of coupled walls. Spalling of concrete cover, buckling of reinforced rods. Large cracks in partition and infill walls, failure of individual infill panels.</p>	<p>DS 3:</p> <p>Δ_u^{inf}</p>	

The definition of the Damage State (DS) has been carried out interpreting and translating through engineering judgment the qualitative terms, *fine cracks*, *cracks* and *large cracks* for non-structural elements, presented in EMS-98 into displacement threshold related to non linear behavior of infills. In particular a building is classified in Grade 1 (DS1) if it exhibits fine cracks in infills. This condition corresponds into mechanical model of building to the overtaking of the cracking displacement to the envelope of infills. Instead Grade 2 and 3, characterize by an increasing level of damage, can be associated to the displacement relative to maximum infills resistance and by the failure of infill, respectively. [Figure 5](#) shows an example of DS1, DS2 and DS3, specifically referred to infills damage classification provided in [Table 2](#); such damage have been observed after the 2012 Emilia earthquake.



(a)



(b)



(c)

Figure 5. Example of damage to infills during the 2012 Emilia earthquake that can be representative of DS1 [from Decanini et al., 2012] (a), DS2, [from EPICentre Field Observation Report No. EPI-FO-290512, 2012] (b), and DS3 [taken by Flavia De Luca] (c).

4 EXACT VULNERABILITY APPROACH

In the following the adopted detailed or *EXACT* vulnerability analysis approach will be illustrated: the simulated design procedure is explained in section 4.1; the adopted numerical model is presented in section 4.2; analysis methodology and obtained results are illustrated in 4.3 and 4.4, respectively.

4.1 Simulated design procedure

Element dimensions are defined through a simulated design procedure according to code prescriptions and design practices in force in Italy between 1950s and 1970s ([Regio Decreto Legge n. 2229, 16/11/1939](#); [Verderame et al., 2010a](#)). The structural configuration follows the parallel plane frames system: gravity loads from slabs are carried only by frames in longitudinal direction. Beams in transverse direction are not present in the internal frames. Element dimensions are calculated according to the allowable stresses method; the design value for maximum concrete compressive stress is assumed equal to 5.0 and 7.5 MPa for axial load and axial load combined with bending, respectively. Column dimensions are calculated according only to the axial load based on the tributary area of each column; beam dimensions and reinforcement are determined from bending due to loads from slabs. Reinforcing bars are smooth and their allowable design stress is equal to 160 MPa. Section dimensions are (30x50) cm² for beams, whereas they are strongly variable for columns, depending on the design axial load and on the selected shape – in this approach column can have square or rectangular section.

4.2 Numerical model

Nonlinear response of RC elements is modeled by means of a lumped plasticity approach: beams and columns are represented by elastic elements with nonlinear rotational hinges at the ends. A three-linear envelope is used, where characteristic points are cracking, yielding and ultimate. Section moment and curvature at cracking and yielding are calculated on a fiber section, for an axial load value corresponding to gravity loads. The behavior is assumed linear elastic up to cracking and perfectly-plastic after yielding. Rotations at yielding and ultimate are evaluated through the formulations given in ([Fardis, 2007](#)). No reduction of ultimate rotation for the lack of seismic detailing is applied, due to the presence of smooth reinforcement ([Verderame et al., 2010b](#)).

Infill panels are modeled by means of equivalent struts. Modeling infills through single compressed struts allow to investigate on the effect of the panels on the global behavior of the analyzed structure (highlight possible brittle failure due to interaction between infill panels and the

surrounding RC elements is beyond the purpose of this paper). The adopted model for the envelope curve of the force-displacement relationship is the model proposed by Panagiotakos and Fardis (Panagiotakos and Fardis, 1996; Fardis, 1997). The proposed force-displacement envelope is composed by four branches, as shown in Figure . The first branch corresponds to the linear elastic behavior up to cracking; the slope of this branch is the elastic stiffness of the infill panel k_{el} , and it can be expressed according to Equation (1), being A_w is the transversal area of the infill panel, G_w the shear elastic modulus and h_w its clear height. If τ_{cr} is the shear cracking stress, the shear cracking strength F_{cr} can be obtained according to Equation (2).

$$K_{el} = \frac{G_w A_w}{h_w} \quad (1)$$

$$F_{cr} = \tau_{cr} A_w \quad (2)$$

The second branch continues up to the maximum strength F_{max} , which can be calculated according to Equation (3). The corresponding displacement Δ_{max} is estimated in the hypothesis that secant stiffness up to maximum is provided by Mainstone's formulation (Mainstone, 1971), assuming that width of the equivalent truss b_w is according to Equation (4), being h_w and d_w the height and the diagonal length of the truss, respectively, and λh is defined according to Equation (5). In Equation (5), E_w and E_c are the elastic Young modulus of the infill panel and of the surrounding concrete, respectively; θ is the diagonal slope of the equivalent truss; t_w is the infill thickness; I_c is the moment of inertia of the adjacent columns. Secant stiffness up to maximum is equal to the expression shown in Equation (6).

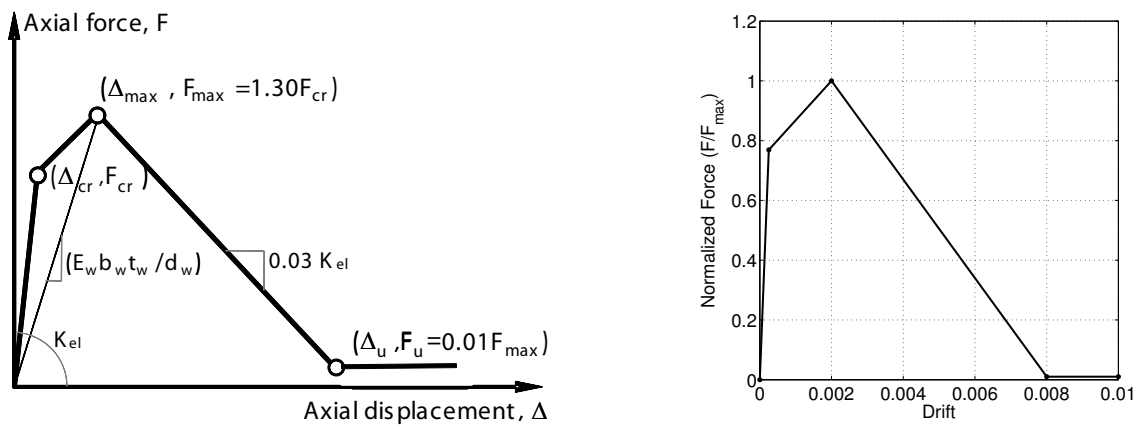


Figure 6. Panagiotakos and Fardis single-strut infill model

$$F_{\max} = 1.30 \cdot F_{cr} \quad (3)$$

$$b_w = 0.175 (\lambda_h h_w)^{-0.4} d_w \quad (4)$$

$$\lambda_h = \sqrt[4]{\frac{E_w t_w \sin(2\theta)}{4E_c I_c h_w}} \quad (5)$$

$$K_{\text{sec}} = \frac{E_w b_w t_w}{\sqrt{L^2 + H^2}} \cos \theta \quad (6)$$

The third branch of the infill envelope is a degrading branch up to the residual strength of the infill panel; its slope (k_{deg}) depends on the elastic stiffness through the parameter α . In literature, authors suggest values in the range [0.005; 0.1] for the parameter α , see Equation (7). Last branch is horizontal; it corresponds to a residual constant strength; residual-to-maximum strength ratio β can be assumed equal to 1-2% (Panagiotakos and Fardis, 1996; Dolšek and Fajfar, 2004a). In this report, the ratio between post-capping degrading stiffness and elastic stiffness (parameter α) is assumed equal to 0.03 (Panagiotakos and Fardis, 1996). The ratio between residual strength and maximum strength (parameter β) is assumed equal to 0.01 (Dolšek and Fajfar, 2004a).

$$K_{\text{deg}} = -\alpha K_{el} \quad (7)$$

4.3 Analysis methodology

Nonlinear static push-over (SPO) analyses are performed on the benchmark buildings both in X and Y direction: the assumed lateral load pattern is proportional to the displacement shape of the first mode and lateral response is evaluated in terms of base shear-top displacement relationship. Structural modeling and numerical analyses are performed through the “PBEE toolbox” software (Dolšek, 2010), combining MATLAB® with OpenSees (McKenna et al., 2004), modified in order to include also infill elements (Ricci, 2010; Celarec et al., 2012).

The lateral response is characterized by a strength degradation due to infill failure; thus a multi-linearization of the pushover curve is necessary and it is carried out by applying the equal energy rule respectively between the initial point and the maximum resistance point, and between the point corresponding to the last infill failure and the point corresponding to the first RC element conventional collapse.

Starting from the multi-linearized capacity curves, IN2 curves (Dolšek and Fajfar, 2008) for the equivalent SDoF systems are obtained by assuming as Intensity Measure (IM) both the elastic

spectral acceleration at the period of the equivalent SDoF system ($S_{ae}(T_{eff})$) and the PGA. An IN2 curve, such as an IDA curve, is a relationship between a Demand Parameter (EDP), e.g. top horizontal displacement, and an IM, e.g. elastic spectral acceleration for a certain period or PGA. If an IN2 curve in terms of top displacement versus PGA is considered, the PGA corresponding to a certain value of top displacement represents the PGA capacity of the structure for that displacement. Thus, the seismic capacity expressed in terms of PGA is defined as the PGA corresponding to the demand spectrum under which the displacement demand is equal to the displacement capacity. In the same way, seismic capacity expressed in term of $S_{ae}(T_{eff})$ can be defined.

Values of $S_{ae}(T_{eff})$ and PGA corresponding to characteristic values of displacement (ductility) demand (including the considered DSs) are calculated, based on the R- μ -T relationships given in (Dolšek and Fajfar, 2004a) for degrading response (Figure 7). It is worth noting that this relation is intended to be used with an idealized elastic spectrum of the Newmark-Hall type.

The strength reduction factor R can be defined as the ratio between the elastic spectral acceleration corresponding to the effective period S_{ae} and the yielding acceleration S_{ay} of the equivalent SDoF. The ductility μ can be expressed as a function of R as shown in Equation (8).

Hence, in the proposed R- μ -T relationship, the ductility μ is linearly dependent on R-factor; the parameter c defines the slope of the R- μ relationship and it depends on the effective period of the structure, the minimum-to-maximum strength ratio r_u and on the characteristic periods of the ground motion T_C and T_D (Dolšek and Fajfar, 2004a). Equation (8) can be rewritten in the form of Equation (9), which can be used for the determination of reduction factors for a given ductility.

$$\mu = \frac{1}{c}(R - R_0) + \mu_0 \quad (8)$$

$$R = c(\mu - \mu_0) + R_0 \quad (9)$$

The proposed R- μ -T relationship has been validated only to a maximum value of the ductility at the beginning of degradation μ_s equal to 2.5 and to a minimum value of r_u equal to 0.25, which may represent some limits of applicability of this law. The central value can be calculated either for the ductility μ at a given reduction factor R or for the reduction factor R for a given ductility μ . These two approaches can lead to different results (Chopra and Chintanapakdee, 2003). In (Dolšek and Fajfar, 2004a), authors demonstrate that the proposed R- μ -T relationship yields larger ductilities for a given reduction factor and, if inverted, a smaller reduction factor for a given ductility, thus

proving the conservativeness of this relation both for performance assessment and design. Furthermore, the authors proved that the ductility at the end of strength degradation μ_u has a negligible influence on the reduction factor R , thus this parameter is not included in the proposed law. The ductility at the beginning of degradation μ_s and the residual-to-maximum strength ratio r_u are essential for the proposed R - μ - T relationship and, thus, IN2 curves are strictly dependent on the parameters μ_s and r_u of the multi-linearized capacity curves.

Moreover, the procedure proposed in (Dolšek and Fajfar, 2005) to improve the accuracy of the displacement demand assessment in the case of low seismic demand is applied. The N2 method is not intended to be used for structures which remain in the (equivalent) elastic region. However, one may wish to compute realistic displacement demand also for acceleration demand $S_{ac}(T)$, which is lower than the yield acceleration S_{ay} of the idealized pushover curve, i.e. for $R < 1$. This goal can be obtained by approximating the first part of the pushover curve by a bilinear curve rather than a linear one and applying specific R - μ - T relationship in this range of behavior, as proposed by Dolšek and Fajfar. The two parts of the bilinear curve are separated by the point $(D_e; F_e)$, which represents the boundary of the initial ideal elastic behavior, and is arbitrarily defined as the crossing point of the radial line with a slope equal to 95% of the initial stiffness of the structure with the computed pushover curve. This improvement of accuracy is applicable to any structural system which is characterized by a pushover curve that substantially deviates from a line in the equivalent elastic region. Elastic spectra used for the construction of the IN2 curves are the demand spectra adopted in Eurocode 8 – type A – for a soil type D (see Figure 3).

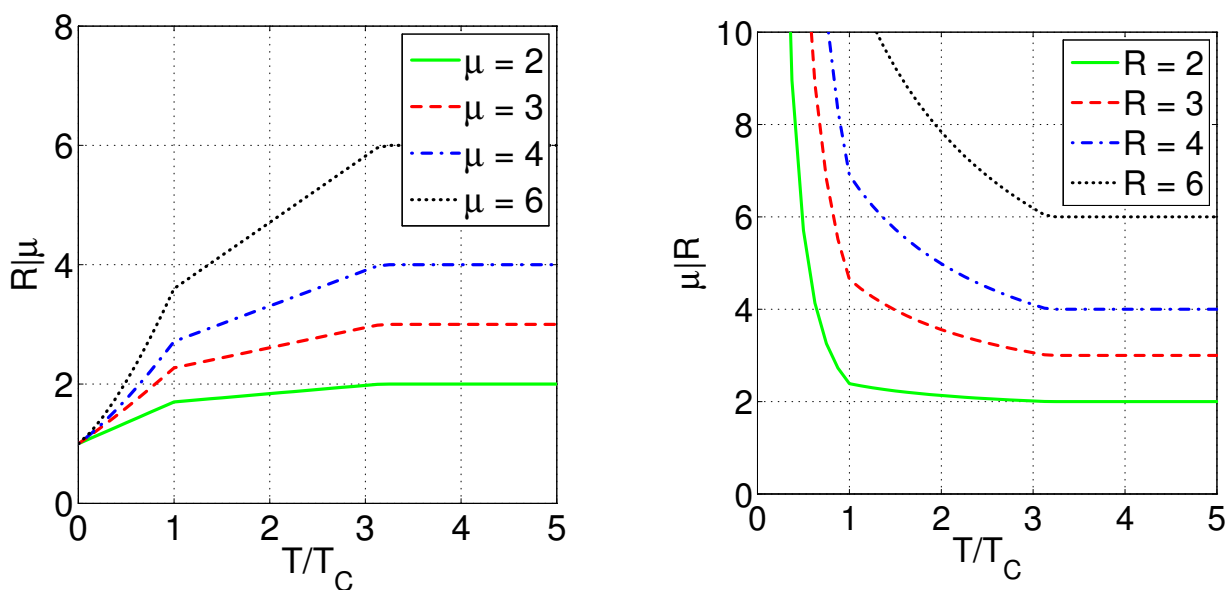


Figure 7. Adopted R - μ - T relationship for infilled frames with $r_u=0.4$, $\mu_s=2.5$, $T_C=0.8s$, $T_D=2s$

4.4 Results

Pushover curves are obtained for the case study buildings in both longitudinal and transverse directions; two- and four-storey case study buildings show a collapse mechanism involving the only first storey in both directions; six-storey building shows a collapse mechanism involving the only second floor in longitudinal direction and first and second floors in the transverse one.

Capacity curves and IN2 curves in terms of $S_{ea}(T_{eff})$ – obtained as explained above – are reported in [Figure 8](#) for each benchmark structure. Capacity curves parameters are also summarized in [Table 3](#), where:

- T_{el} is the elastic period of the structure;
- T_{eff} is the effective period of the structure;
- μ_s is the ductility at the beginning of the degradation;
- $C_{s,max}$ is the maximum strength of the equivalent SDoF system, before the strength degradation due to infills;
- $C_{s,min}$ is the minimum strength of the equivalent SDoF system, after the strength degradation due to infills;
- r_u is the residual-to-maximum strength ratio;
- M^* is the effective mass.

Moreover, seismic capacity expressed in term of $S_{ae}(T_{eff})$ is reported for each DS and for each case study. Finally, in [Table 4](#), displacement capacities of the equivalent SDoF corresponding to the achievement of the analyzed DSs are reported.

Table 3. Capacity curves parameters and $S_{ae}(T_{eff})$ capacity – Detailed approach

Number of storeys	direction	Capacity curves' parameters							$S_{ae}(T_{eff})$ capacity		
		T_{el} [s]	T_{eff} [s]	μ_s	$C_{s,max}$ [g]	$C_{s,min}$ [g]	r_u	M^* [t]	DS1 [g]	DS2 [g]	DS3 [g]
2	x	0.0818	0.1088	2.5649	0.9501	0.1999	0.2104	364	0.5537	1.0475	1.1261
	y	0.1056	0.1438	2.8602	0.5863	0.1815	0.3096	370	0.3222	0.6605	0.8046
4	x	0.1467	0.1878	3.0368	0.5446	0.2129	0.391	633	0.2690	0.6457	0.8121
	y	0.2013	0.2525	2.8123	0.3294	0.1477	0.4485	604	0.1540	0.4100	0.5434
6	x	0.2201	0.2675	3.3837	0.3857	0.2368	0.6139	879	0.1751	0.4615	0.6914
	y	0.3074	0.3435	2.1102	0.2169	0.0992	0.4574	841	0.1078	0.2788	0.3843

Table 4. Displacement capacity of the equivalent SDoF – Detailed approach

S_d	DS1	DS2	DS3	S_d	DS1	DS2	DS3
Direction x	[cm]	[cm]	[cm]	Direction y	[cm]	[cm]	[cm]
2 storeys	0.098	0.581	3.161	2 storeys	0.101	0.604	3.201
4 storeys	0.158	1.017	3.183	4 storeys	0.168	1.100	3.960
6 storeys	0.225	1.262	3.509	6 storeys	0.258	1.240	3.396

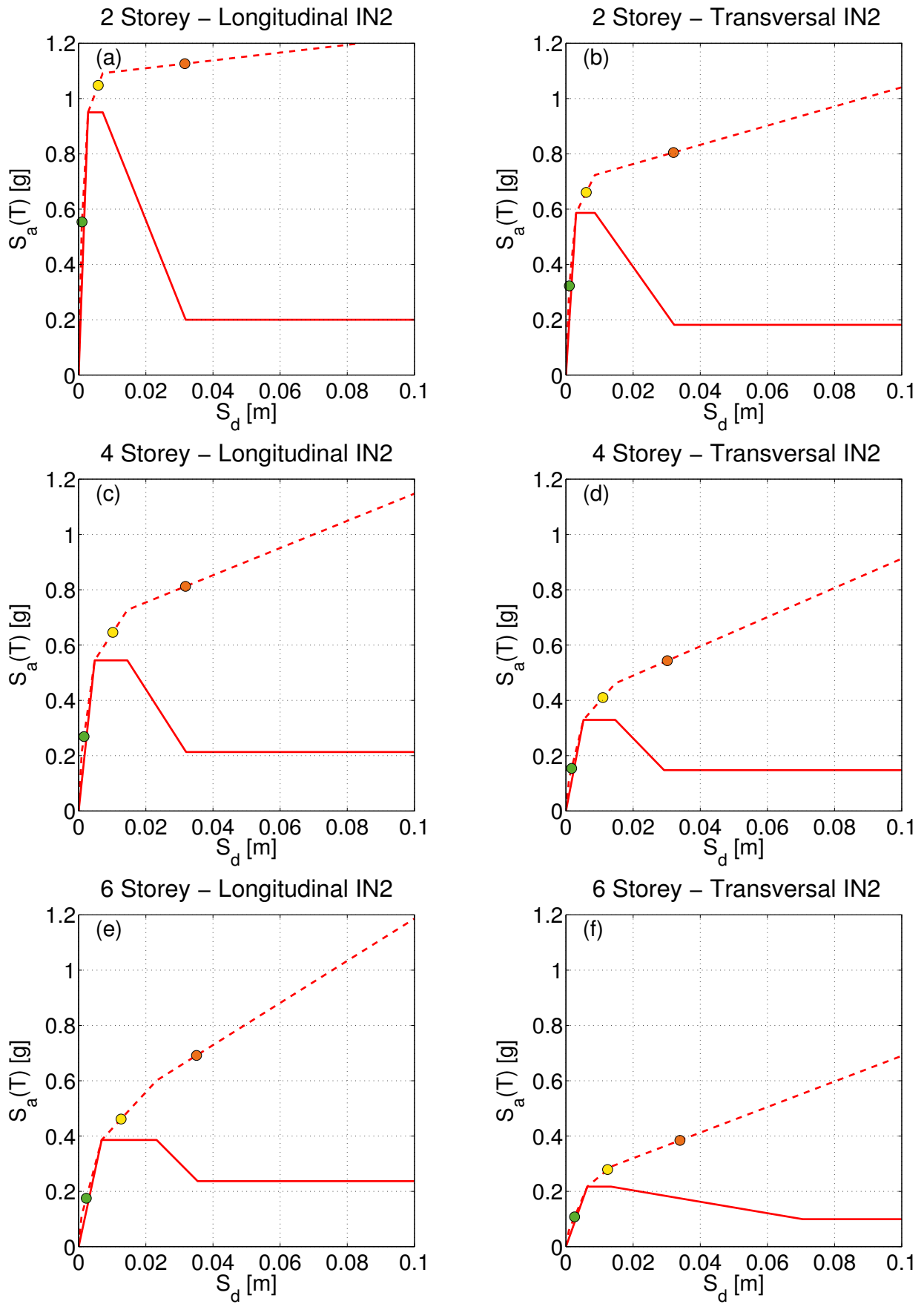


Figure 8. Multi-linearized capacity curves and IN2 curves in terms of $S_{ae}(T_{eff})$ – Detailed approach

5 POST VULNERABILITY APPROACH

POST (**P**ush**O**ver on **S**hear **T**ype models) is a simplified method for vulnerability assessment of reinforced concrete buildings, employing a simulated design procedure to evaluate the building structural characteristics based on few data such as number of storeys, global dimensions and type of design, and on the assumption of a Shear Type behavior to evaluate in closed form the non-linear static response. Hence, the N2 method is applied and the seismic capacity in terms of elastic spectral acceleration at the period of the equivalent SDOF system and of the corresponding Peak Ground Acceleration is evaluated, based on the displacement (ductility) capacity at the Damage State of interest. POST is implemented in MATLAB® code, including a user interface, (see [Figure 9](#)).

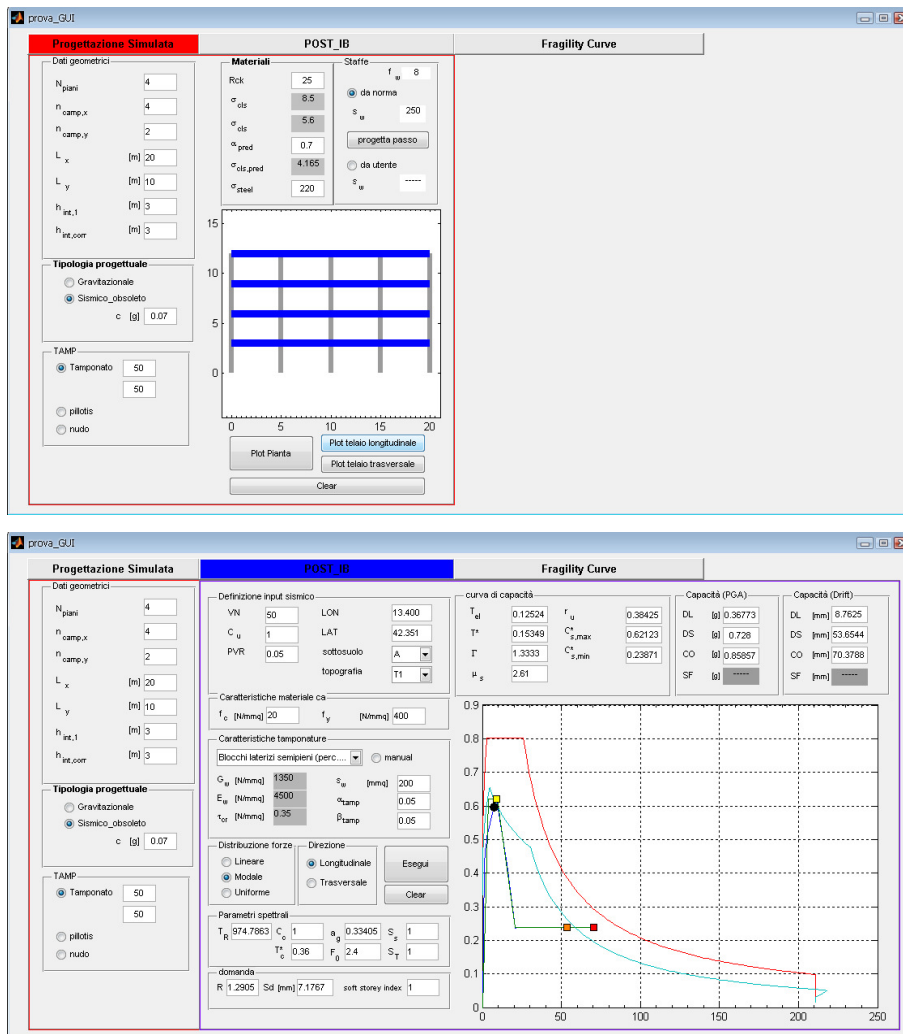


Figure 9. POST user interface.

5.1 Input data

The first step of the procedure consists of the definition of input data. These data include:

- global geometrical parameters;
- distribution of infill panels;
- type of design and values of allowable stresses to be employed in the simulated design procedure;
- material characteristics;
- data for the definition of seismic hazard.

Considered buildings are rectangular in plan. Hence, the parameters needed to completely define the global building geometry include: number of storeys, plan dimensions in longitudinal (X) and transverse (Y) directions, number of bays in X and Y, height of the bottom storey, height of upper storeys. Hence, a possible irregularity in interstorey height (often due to architectonic or functional reasons) is considered.

The presence of infill panels can be defined according to three different options: (i) Uniformly infilled building, (ii) Pilotis building or (iii) Bare building. The opening percentage can also be defined, both in bottom infill panels (case i) and in upper infill panels (cases i and ii). If present, infill panels are regularly distributed in plan in all the external frames in X and Y directions.

The design can be based on gravity loads only or on gravity and seismic loads. If the design is seismic, the base shear coefficient prescribed by code (to be employed in the simulated design procedure) is needed as input. Values of allowable stress for concrete and steel are also defined.

Material characteristics are defined, namely the concrete compressive strength, the steel yield strength and the infill characteristics (if infill panels are present). The latter include the thickness of infill panels, the infill mechanical characteristics (shear cracking strength, shear elastic modulus and Young's elastic modulus) and parameters α and β , respectively representing the ratio between post-capping degrading stiffness and elastic stiffness and the ratio between residual strength and maximum strength, according to the model proposed by Panagiotakos and Fardis ([Panagiotakos and Fardis, 1996](#); [Fardis, 1997](#)). Hence, the envelope of the lateral force displacement relationship of infill panels can be completely defined, according to the adopted model. Values of infill mechanical characteristics from the Italian code ([CS. LL. PP., 2009](#)) are proposed as default values for different infill typologies.

Results reported in the following were obtained by adopting the same data described at Sections 4.1 and 4.2 as input data for global geometrical parameters, distribution of infill panels, type of

design and values of allowable stresses to be employed in the simulated design procedure, and material characteristics.

5.2 Simulated design procedure

The simulated design procedure adopted herein (Verderame et al., 2010a) is based on the compliance with past code prescriptions and design practices for Italian RC buildings. Hence, the allowable stresses method is followed.

First, design loads are defined. As far as gravity loads are concerned, dead loads are evaluated from a load analysis, whereas live loads are evaluated from past code prescriptions for ordinary structures (e.g., 2 kN/m²). Lateral loads (evaluated if the selected type of design is “seismic”) are calculated based on the assigned base shear coefficient (ratio between the design base shear and the weight of the structure). Typical values for this coefficient were, for instance, 0.07 or 0.10, according to the category of the seismic zone.

Then, element dimensions are evaluated. To this aim, according to past design practices, column area is determined as the ratio between the axial load (evaluated referring to the area of influence of each column) and the allowable stress of concrete. In seismic design, the latter was typically multiplied by a coefficient γ lower than 1, roughly accounting for combined axial load and bending action acting on the column due to lateral loads (Pecce et al., 2004). Hence, γ was typically assumed equal to 1 in gravity load design. Coefficient γ is given as an input for the simulated design procedure. The column section is then determined from the calculated area, starting from a width equal to 30 cm and considering a maximum height of 70 cm. If the calculated area is higher than cm², column width is increased from 30 to 35 cm, and so on. An upper approximation of 5 cm is considered for the determination of section height. The beam width is given equal to 30 cm and the corresponding height is calculated based on the maximum bending moment acting on the beam for gravity loads from slabs; this moment is calculated with a formulation accounting in a simplified way for the element constraint scheme. Finally, column dimensions are checked to avoid cross-section variation higher than 10 cm between two adjacent storeys.

Once column and beam dimensions have been calculated, reinforcement in columns is designed. Beam reinforcement is not designed since in the assumed Shear Type model the behavior of beam elements has not to be modeled.

As far as gravitational design is concerned, the design of column reinforcement is based on the minimum amount of longitudinal reinforcement geometric ratio prescribed by code (e.g., 0.8% of the minimum concrete area according to RDL 2229 (1939), or 0.6% according to DM 3/3/1975)).

Once the minimum area of reinforcement has been determined, a set of possible values of bar diameter is considered and the combination of (even) number and diameter of bars providing the best upper approximation is chosen. Hence, bars are distributed along the periphery of the section as uniformly as possible.

In seismic design, storey shear forces are evaluated from lateral forces, which are calculated as a fraction of the weight of the structure, based on the assigned base shear coefficient. Hence, the distribution of the storey shear among the columns of the storey is based on the ratio of inertia of the single column versus the sum of inertia of all the columns at the considered storey (Shear Type element model). The bending moment acting at the ends of each column is obtained multiplying the corresponding shear force by half of the column height, according to the assumed Shear Type model; the axial load is calculated from gravity loads, given by the sum of gravity loads and of a fraction of live loads (30%), always based on the area of influence of the column. Then, based on the assigned values of allowable stress for steel and concrete, the reinforcement area is designed to provide a flexural strength (according to the allowable stresses method) not lower than the bending moment from design. Again, the combination of number and diameter of bars providing the best upper approximation is chosen provided at least two bars per layer. The described procedure is carried out in both directions. Hence, the total amount of longitudinal reinforcement is compared with the minimum amount prescribed by the considered code; the maximum between these values is assumed.

5.3 Characterization of nonlinear response

Based on the assumed Shear Type model, the lateral response of the structure under a given distribution of lateral forces can be completely determined based on the interstorey shear-displacement relationships at each storey. Hence, the nonlinear response of column and infill elements has to be determined.

The nonlinear behavior of each column element is characterized as a $T(\Delta)$ relationship evaluated from the corresponding $M(\theta)$ relationship, consistent with the Shear Type assumption.

The moment-rotation envelope is calculated assuming a shear span equal to half of the column height ($L_V = h/2$). A tri-linear envelope for is assumed, with three characteristic points: cracking, yielding and ultimate condition. Behavior is linear elastic up to cracking and perfectly-plastic after yielding.

Moment and rotation at cracking are evaluated based on first principles, assuming a linear elastic section behavior up to this point.

Moment and section curvature at yielding are calculated in closed form by means of the first principles-based simplified formulations proposed in (Biskinis and Fardis, 2010). Hence, rotations at yielding (θ_y) and ultimate (θ_u) are evaluated according to (Biskinis and Fardis, 2010) and (Biskinis and Fardis, 2010), respectively. The type of reinforcement is given as input, too; if smooth bars are present, no reduction for the lack of seismic detailing is applied (Verderame et al., 2010b). Then, the relationship between the displacement and the shear for each column is evaluated from the relationship between the chord rotation and the end moment

Lateral force-displacement relationships for infill panels are evaluated from the model proposed by Panagiotakos and Fardis (Panagiotakos and Fardis, 1996; Fardis, 1997), based on previously defined data (panel thickness, infill mechanical characteristics and model parameters α and β) and evaluating clear dimensions of the panel considering section dimensions of surrounding beams and columns.

At each storey, the relationship between the interstorey displacement and the corresponding interstorey shear is evaluated considering all the RC columns and the infill elements (if present) acting in parallel. To this aim, displacement values corresponding to characteristic points of lateral force-displacement envelopes of RC columns and infill elements are sorted in a vector; then, for each of these displacement values the corresponding shear forces provided by each element are evaluated and summed. In this way, a multi-linear storey shear-displacement relationship is obtained. The illustrated procedure is carried out in both building directions.

5.4 Seismic assessment

Once the interstorey shear-displacement relationship at each storey has been defined, the base shear-top displacement relationship representing the lateral response of the Shear Type building model – under a given distribution of lateral forces – can be evaluated through a closed-form procedure.

First, the fundamental period of vibration and the corresponding lateral displacement shape are evaluated by means of an eigenvalue analysis. To this aim, mass and stiffness matrices of the Shear Type model are easily constructed; elastic stiffness at each storey is calculated as the ratio between force and displacement values corresponding to the first point of the multi-linear envelope representing the interstorey shear-displacement relationship.

Hence, a linear, uniform or 1st mode lateral displacement shape is chosen and the corresponding lateral load shape is determined.

Once the shape of the applied distribution of lateral forces is given, the shape of the corresponding distribution of interstorey shear demand can be determined, too. A normalized distribution of interstorey shear demand is assumed and the ratios between such demand forces and the corresponding interstorey shear strengths (i.e., maximum force values of the interstorey shear-displacement relationships) are calculated. Hence, the storey characterized by the maximum value of this ratio will be the first (and only) to reach its maximum resistance (with increasing lateral displacement). Hence, if infill elements are present at that storey, leading to a degrading post-peak behavior of the interstorey shear-displacement relationship, that storey will also be the first (and only) to start to degrade, thus controlling the softening behavior of the structural response. Moreover, the peak of resistance of the pushover curve can be calculated from the interstorey shear resistance of the same storey, based on the constant ratio between the interstorey shear at that storey and the base shear. As a matter of fact, due to the constant shape of the lateral force distribution, such a ratio can be calculated at each storey and remains constant at each step of the pushover curve.

Therefore, the pushover curve can be evaluated by means of a force-controlled procedure up to the peak and by means of a displacement-controlled procedure after the peak. In the latter phase, the evaluation of the response is based on the interstorey shear-displacement relationship of the storey where the collapse mechanism has taken place. At each step, the top displacement is calculated as the sum of the interstorey displacement at each storey, evaluated as a function of the corresponding interstorey shear demand, whereas the base shear is given by the sum of lateral applied forces. If the storey where the collapse mechanism takes place is characterized by a softening post-peak behavior, during the post-peak phase in the remaining $N-1$ storeys (where N is the number of storeys) the interstorey shear will decrease starting from a pre-peak point of the interstorey shear-displacement relationship; hence, the corresponding displacement will decrease, too, following an unloading branch. An unloading stiffness equal to the elastic stiffness is assumed. [Figure 10](#) reports a schematic representation of the described procedure.

Following this procedure, the pushover curve can be completely determined in both directions.

Once the interstorey shear-displacement relationship at each storey has been defined, the base shear-top displacement relationship representing the lateral response of the Shear Type building model – under a given distribution of lateral forces – can be evaluated through a closed-form procedure. Once the shape of the applied distribution of lateral forces is given, the shape of the corresponding distribution of interstorey shear demand can be determined, too.

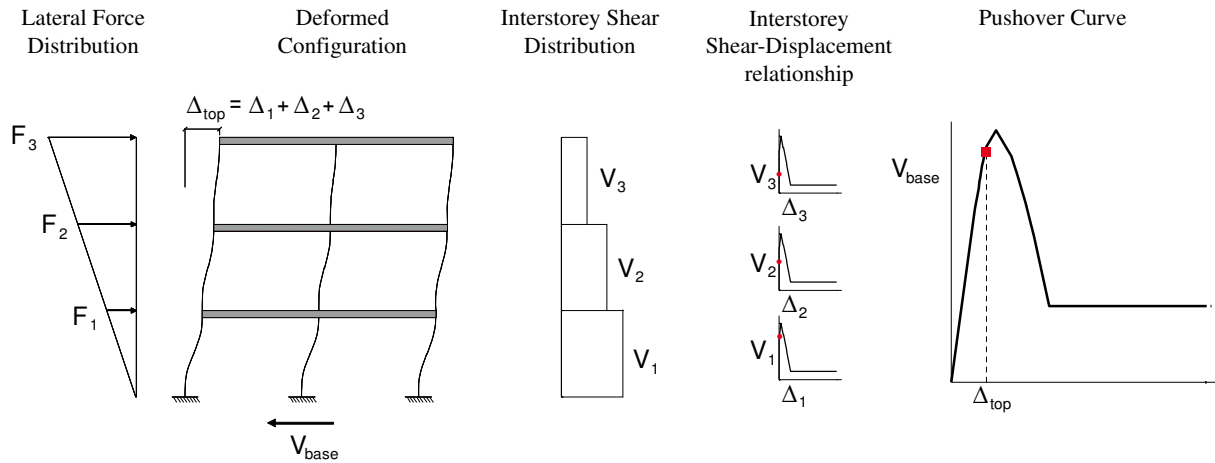


Figure 10. Calculation of pushover curve

Therefore, the pushover curve can be evaluated by means of a force-controlled procedure up to the peak, and by means of a displacement-controlled procedure after the peak. At each step, the top displacement is calculated as the sum of the interstorey displacement at each storey, evaluated as a function of the corresponding interstorey shear demand, whereas the base shear is given by the sum of lateral applied forces. If the storey where the collapse mechanism takes place is characterized by a softening post-peak behavior, during the post-peak phase in the remaining $N-1$ storeys (where N is the number of storeys) the interstorey shear will decrease starting from a pre-peak point of the interstorey shear-displacement relationship; hence, the corresponding displacement will decrease, too, following an unloading branch. An unloading stiffness equal to the elastic stiffness is assumed.

Once the pushover curve has been determined, the displacement capacity is evaluated for the assumed Damage States, based on the shear displacement relationships assumed for structural and/or non-structural (as in this case, see Section 3) elements. Then, seismic capacity is evaluated and IN2 curves are constructed according to the same procedure described at Section 4.3.

Capacity curves and IN2 curves in terms of $S_{ea}(T_{eff})$ – obtained as explained above – are reported in Figure 11 for each benchmark structure. Capacity curves parameters are also summarized in Table 5. Seismic capacity expressed in term of $S_{ae}(T_{eff})$ is reported for each DS and for each case study. Finally, in Table 6, displacement capacities of the equivalent SDoF corresponding to the achievement of the analyzed DSs are reported.

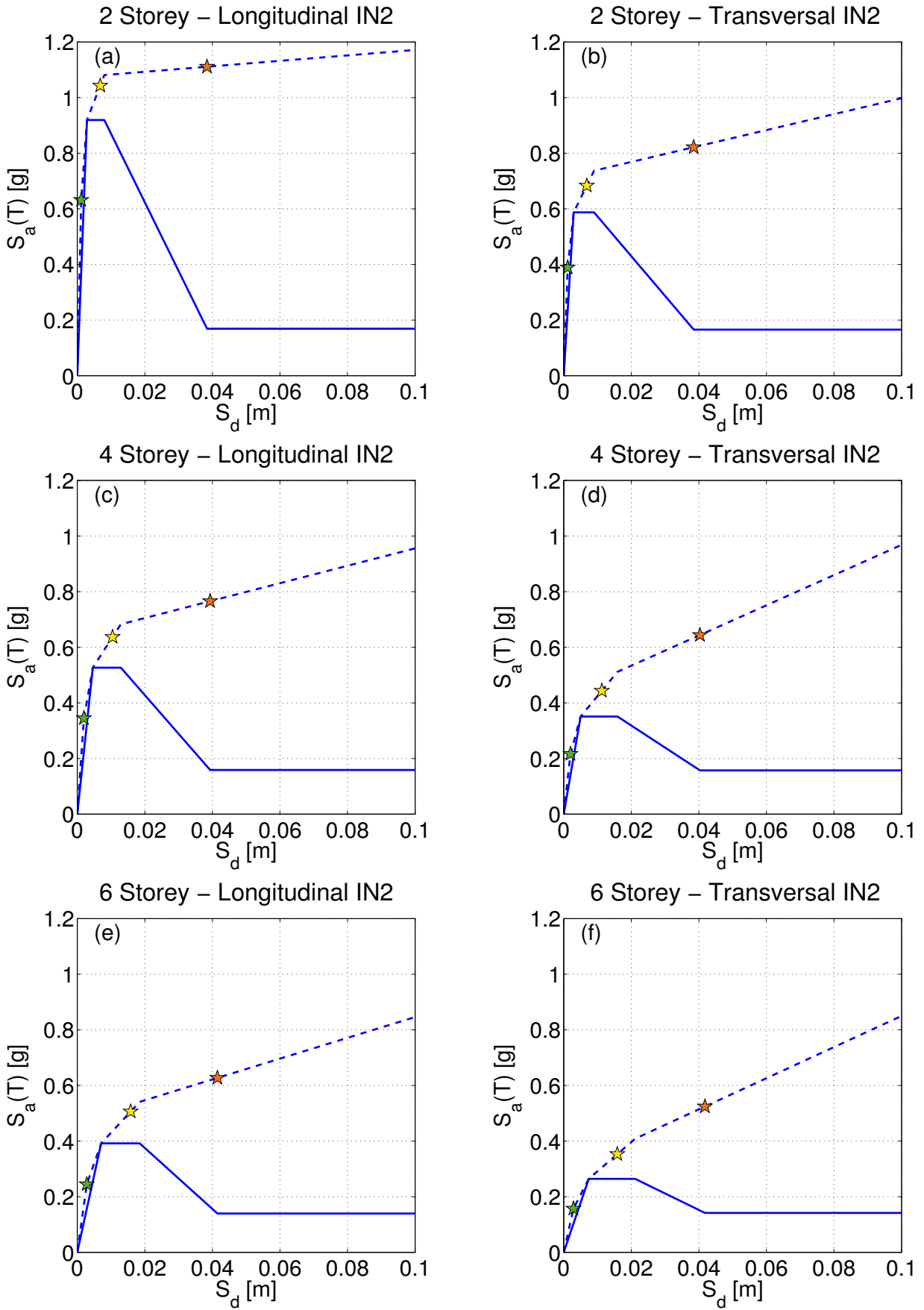


Figure 11. Multi-linearized capacity curves and IN2 curves in terms of $S_{ac}(T_{eff})$ – *POST* approach

Table 5. Capacity curves parameters and $S_{ae}(T_{eff})$ capacity – POST approach

Number of storeys	direction	Capacity curves' parameters							$S_{ae}(T_{eff})$ capacity		
		T_{el}	T_{eff}	μ_s	$C_{s,max}$	$C_{s,min}$	r_u	M^*	DS1	DS2	DS3
		[s]	[s]		[g]	[g]		[t]	[g]	[g]	[g]
2	X	0.084	0.112	2.795	0.919	0.169	0.184	380	0.632	1.043	1.111
	Y	0.108	0.142	3.052	0.587	0.166	0.282	380	0.389	0.683	0.822
4	X	0.147	0.187	2.809	0.527	0.159	0.302	672	0.345	0.637	0.766
	Y	0.187	0.239	3.183	0.351	0.157	0.448	670	0.217	0.443	0.644
6	X	0.210	0.269	2.617	0.392	0.140	0.356	963	0.245	0.506	0.627
	Y	0.265	0.336	2.863	0.264	0.142	0.537	958	0.157	0.353	0.524

Table 6. Displacement capacity of the equivalent SDoF – POST approach

S_d	DS1	DS2	DS3	S_d	DS1	DS2	DS3
Direction x	[cm]	[cm]	[cm]	Direction y	[cm]	[cm]	[cm]
2 storeys	0.118	0.679	3.841	2 storeys	0.118	0.681	3.847
4 storeys	0.196	1.045	3.934	4 storeys	0.198	1.127	4.032
6 storeys	0.281	1.581	4.149	6 storeys	0.287	1.586	4.179

6 FAST VULNERABILITY APPROACH

The *FAST* approach can be located in the main framework of the rapid large-scale assessment method, as it was briefly outlined in section 3. The application of such methodology asks for very basic information and data on the building stock of the area to be studied: number of stories, age of construction, design code (e.g., according to the evolution of the seismic classification), typical structural and nonstructural material mechanical properties at the time (e.g., [Verderame et al., 2001](#); [STIL, 2012](#); [CS. LL. PP., 2009](#); [Augenti, 2009](#)).

The *FAST* approach has at its basis a simplified procedure for the definition of the capacity curve of existing buildings in both the case of seismic design according to old codes or gravity load design (substandard RC buildings). In the first case the lateral force of the bare structure can be defined by means of the spectral acceleration employed at the time of construction ([De Luca et al., 2012](#)) and accounting for overstrength factors ([Borzi and Elnashai, 2000](#); [Galasso et al., 2011](#)).

In the case of design for gravity load only, also in this case it is necessary to employ a simulated design procedure, in analogy with the approach followed for the other methods described above.

On the other hand, it should be noted that a simulated design procedure can be a suitable solution also for the case of buildings designed for seismic loads according to old codes in the case of low or mid rise buildings and low or medium hazard at the site (low values of spectral accelerations). In fact, in such cases the gravity load design can still rule the lateral strength of the building. There is another key issue that makes simulated design a reliable solution; this approach accounts for overstrengths sources explicitly. For example it is possible to account for overstrengths due to the minimum reinforcement ratios provided by codes or in general produced by the application of practical design rules, avoiding the problem to choose a proper “blind” overstrength factor. In general, without any simulated design procedure, the easiest way to consider overstrengths is to consider the overstrength factor caused by the difference between nominal and mean properties of materials ([Borzi and Elnashai, 2000](#); [Galasso et al., 2011](#)), discarding other significant sources of overstrengths.

In the following, it is synthetically discussed the simplified simulated design procedure adopted in this study and suitable to carry out the lateral load strength of the bare structure for the case of gravity load design.

6.1 Simplified simulated design procedure

The simulated design shown herein should be considered as a simplified procedure derived from the detailed approach described in (Verderame et al., 2010a).

Given the area in plan of the building, (A_b), defined the number of storeys, (n), dead loads (g), and live loads (q) per square meters, every storey will be characterized by a gravity load evaluated according to Equation (10); while the whole building will be characterized by a total gravity load equal to the expression provided in Equation (11).

$$p = (g + q)A_b \quad (10)$$

$$P_i = \sum_i^n (g + q)A_b \quad (11)$$

Given an average dimension of the bays' length, (l), (e.g., Bal et al., 2007), it is possible to define the average area of influence of the columns, specializing such evaluation to their position in plan (central, lateral, or corner). Once the area of influence of the central column $A_{inf}^j = l^2$ is defined, for lateral and corner columns the value will be equal to 50% and 20% of A_{inf}^j , respectively.

The previous evaluation allows computing the axial load on the j^{th} column of i^{th} storey according to Equation (12), in which α is equal to 1.00, 0.50, and 0.25 in the cases of central, lateral and corner columns. The section area, a^2 , of the columns (making the simplified hypothesis of square sections, with base and height equal to a) can be evaluated as a function of the design allowable stress, σ_c , as shown in Equation (13).

$$N_i^j = \sum_i^n (g + q) \cdot \alpha \cdot A_{inf}^j \quad (12)$$

$$A_{c,i}^j = a^2 = \frac{\sum_i^n (g + q) \cdot \alpha \cdot A_{inf}^j}{\sigma_c} \quad (13)$$

The longitudinal reinforcement, in turn, can be computed considering minimum code prescriptions or typical building practice; the latter can be expressed as a percentage of the minimum area necessary for the square section (a^2), in the following referred as ρ_l .

The flexural capacity of such columns can then be defined according to Equation (14), being β a coefficient that accounts for reinforcement distribution in the section (e.g. equal to 0.5 in the simplest case of only two registers), and k that accounts in a simplified hypothesis the distance

between the registers. Given the flexural strength of the generic column, it is possible to determine its plastic shear at the j^{th} storey according to Equation (15), in which L_v is the shear span length, taken as one half of the interstorey height h_{int} (e.g., Bal et al. 2007).

$$M_{Rc,i}^j = \frac{N_{c,i}^j \cdot a}{2} \cdot \left(1 - \frac{N_{c,i}^j}{f_c \cdot a^2}\right) + \beta \cdot [\rho_s \cdot (a^2)] \cdot f_y \cdot k \cdot a \quad (14)$$

$$V_{plc,i}^j = \left[\frac{N_{c,i}^j \cdot a}{2} \cdot \left(1 - \frac{N_{c,i}^j}{f_c \cdot a^2}\right) + \beta \cdot \rho_s \cdot (a^2) \cdot f_y \cdot k \cdot a \right] \cdot \frac{1}{L_v} \quad (15)$$

The storey plastic shear is evaluated as the sum of the plastic shears of each column. The lateral strength of the bare structure can be defined as the plastic shear of the first storey (V_y), according to the hypothesis discussed in the next section (first storey plastic mechanism).

6.2 Evaluation of the approximate capacity curve of RC infilled building

The approximate estimation of lateral strength for existing RC buildings can be carried out in the case of infilled structures; thus accounting for the structural contribution provided by infills. The *FAST* vulnerability approach allows an evaluation of PGA capacity for the three damage states of EMS-98 thanks to: (i) a simplified definition of a capacity curve of a RC infilled building and (ii) an empirical-mechanical interpretation of damage states according to EMS98 scale.

The simplified capacity curve of a fully infilled RC building can be represented by quadrilinear backbone (Dolsek and Fajfar 2004a), characterized by an initial elastic plastic backbone (with the maximum base shear strength V_{max}) followed by a softening branch up to the minimum base shear strength (V_{min}). In the *FAST* approach the softening branch is characterized by a drop. The latter is a simplified hypothesis respect to the idealized backbone provided by *EXACT* and *POST* approaches and refers to a significant brittle behavior of the infills.

Figure 12 shows a qualitative example of the approach followed. In Figure 12(a), the typical shape of a pushover curve on infilled RC structures is shown with a qualitative example of the contribution provided by infills and RC frames. The idealized capacity curve is shown in Figure 12(b) and 12(c), respectively in the base shear displacement format and acceleration displacement response spectra (ADRS) format.

The simplified capacity curve of infilled RC structures asks for the definition of four characteristic points. According to the representation in Figure 12(c), the capacity curve in the ADRS format can be defined through the definition of four parameters:

- $C_{s,\text{max}}$, the spectral acceleration of the equivalent SDOF at the attainment of V_{max} ;

- $C_{s,min}$, the spectral acceleration of the equivalent SDOF at the attainment of the plastic mechanism of the structure (at which all the infills of the storey involved in the mechanism have attained their residual strength);
- $T_{1,inf}$, the equivalent fundamental period of the infilled RC structures;
- μ_s , the available ductility up to the beginning of the degradation of the infills.

In Equations (16) to (18) the formulations assumed for the definition of the first three parameters of the approximate infilled capacity curve are shown, while the value of μ_s was assumed equal to 2.5. The latter assumption was made through a comparison with detailed assessment studies available in literature on gravity load designed buildings (Ricci, 2010; Manfredi et al, 2012).

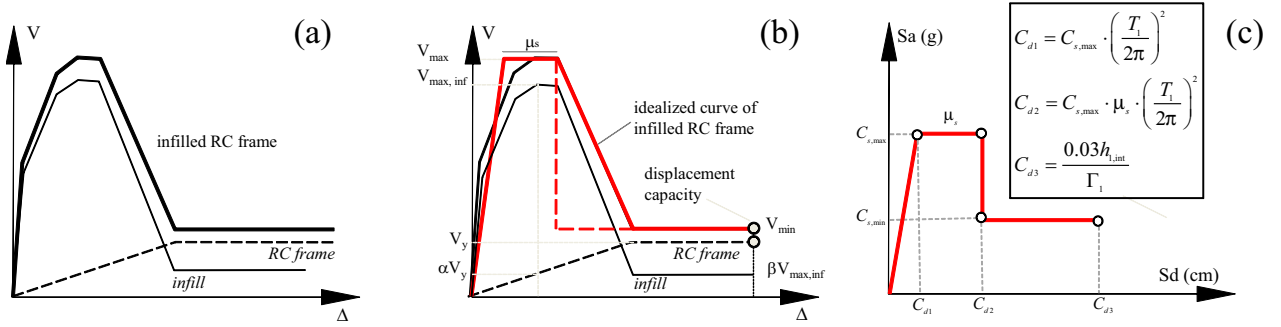


Figure 12. Example of infilled RC frame capacity curve (a), and its quadrilinear idealization in the base shear displacement (b).

$$C_{s,max} = \frac{V_{max}}{\Gamma_1 m_1} = \frac{V_{max,inf} + \alpha V_y}{\Gamma_1 m_1} = \frac{\tau_{max} \cdot A_{inf} + \alpha V_y}{\Gamma_1 m_1} = \frac{\tau_{max} \cdot \rho_w \cdot A_b}{(n \cdot m \cdot A_b \cdot \lambda)} + \alpha C_s = \frac{\tau_{max} \cdot \rho_w}{n \cdot m \cdot \lambda} + \alpha C_s \quad (16)$$

$$C_{s,min} = \frac{V_y + \beta V_{max,inf}}{\Gamma_1 m_1} \quad (17)$$

$$T_{1,inf} = k_1 \cdot T_{el,inf} = k_1 \cdot 0.002 \frac{H}{\sqrt{\rho_w}} \quad (18)$$

$V_{max,inf}$ is the maximum base shear provided by the infills; τ_{max} is the maximum shear stress of the infills, ρ_w is the ratio between the infill area (evaluated along one of the principal directions of the building), and the building area A_b , n is the number of storeys, m is the medium storey mass normalized by the building area (e.g. equal to $0.8t/m^2$ for residential buildings) and λ is a coefficient

for the evaluation of the first mode participant mass respect to the total mass of the MDOF (CEN 2004), equal to 0.85 for buildings with more than three storeys and 1.0 otherwise. Coefficient α and β , account, respectively, for the RC elements' contribution at the attainment of $V_{max,inf}$ and for the residual strength contribution of the infills at the attainment of the plastic mechanism of the RC structure, see Figure 12(a).

Equations (16) and (17) are evaluated in the hypothesis of the attainment of a soft storey plastic mechanism (e.g., ground level) of the structures, see also the previous subsection. Such hypothesis is justified by the fact that in the case of substandard existing buildings (without any capacity design), storey strength and stiffness of the RC structure has a negligible influence if compared to the contribution of the infills (Dolce et al., 2005). In particular, for fully infilled RC buildings, storey strength and stiffness is approximately constant along the height of the building. Thus, considering the typical inverted triangular distribution of lateral force method (first mode distribution), damage is concentrated at the first storey (given its higher storey shear). The subsequent strength drop, caused by brittle nature of infills, finally leads to a soft storey ductile mechanism governed by first storey RC columns (Dolce et al., 2005).

The latter observation justifies also the assumption on the ultimate displacement capacity of the infilled frame ($C_{d,inf}$) through the evaluation of the typical drift at which columns attains their ultimate chord rotation (e.g., approximately equal to 3%).

The fundamental period $T_{1,inf}$, to be employed in the definition of the capacity curve, is an effective period according to the piecewise linearization of the infilled pushover curve provided by Dolsek and Fajfar (2004a). In literature are available formulation for the elastic initial periods of infilled RC buildings (Ricci et al., 2011b); thus in this fast vulnerability approach it is necessary to evaluate a coefficient k_I for the definition of an approximate ratio between elastic initial period ($T_{el,inf}$) and $T_{1,inf}$, as shown in Equation (18). The period coefficient k_I is equal to 1.4 (Manfredi et al, 2012).

For the evaluation of the capacity curves in Figure 12 the subsequent assumptions have been considered. α and β coefficient have been considered equal to 0.5 and 0, respectively. The value of τ_{max} was chosen equal to $1.3 \cdot \tau_{cr}$, according to Fardis (1997) and assuming $\tau_{cr}=0.33$ MPa (see Table 1). The geometric percentage of infilled area respect to the global plan extension (ρ_w) is equal to 0.028 and 0.017 in longitudinal and transverse direction, as shown in Table 1.

The evaluation of $C_{s,\min}$ was made according to the simulated design procedure described in the previous section. The coefficient Γ_1 for the evaluation of the ultimate displacement capacity, C_{d3} in Figure 12(c), was chosen equal to the C_0 values suggested in ASCE/SEI 41-06 (2007).

6.3 Seismic assessment

The definition of an infilled capacity curve allows, in turn, the definition of the IN2 curve according to Dolsek and Fajfar (2004a) $R-\mu-T$ relationship for infilled RC structures. The hypothesis made on the drop of the capacity curve does not affect the evaluation of the corresponding IN2, since this parameter was considered not be significant in the regression made for the determination of the relationship (see section 4).

The empirical-mechanical interpretation of damage states in terms of interstorey drift (IDR), and consequently in terms of equivalent SDOF displacement, (Sd) can be defined according to the classification of the EMS98 scale (Grunthal, 1998). Once such interpretation is defined the simplified approach aimed at determining the IN2 curves allows the evaluation of damage states in terms of $Sa(T)$ and PGA .

The evaluation of the equivalent SDOF displacement, given the specified DS level ($S_{d|DS_i}$) can be made as function of the storey IDR at which the specific DS is attained. In fact, once the $IDR_{|DS_i}$ is computed, the roof displacement can be defined through a deformed shape defined *a priori*. The switching from roof displacement to $S_{d|DS_i}$ is made through Γ_1 defined according to the same approximate hypothesis showed previously (ASCE/SEI 41-06, 2007). The IN2 curve in terms of $Sa(T)$ allows the definition of the spectral acceleration characteristic of each damage state ($Sa(T)_{|DS_i}$). Finally, a scaling of $Sa(T)_{|DS_i}$ in $PGA_{|DS_i}$, according to the spectral shape considered, completes the procedure.

The definition of $IDR_{|DS_i}$, according to EMS98 is made for the only damage states characterized by a specific infill damage level. In particular such procedure can be pursued up to DS3:

- DS1: *Fine cracks in partitions and infills*. This DS is defined by the end of the phase in which infills are characterized by an elastic, uncracked stiffness. The $IDR_{|DS_1}$ could be evaluated as the drift characterizing the attainment of the cracking shear in the infill backbone (Fardis, 1997). Notwithstanding the value of a pure mechanical approach, in this approximate framework the IDR of the first storey at the specific damage level has been defined on experimental basis (Colangelo, 2012). Thus the $IDR_{|DS_1}$ for the first storey is assumed equal to

0.0003. It is worth to note that such experimental value is similar to that computed on pure mechanical basis assuming typical infill characteristics of residential buildings (e.g., clay hollow bricks).

- DS2: *Cracks in partition and infill walls, fall of brittle cladding and plaster.* Crack pattern of the infill is typical of their theoretical post-cracking behavior up to the attainment of the peak strength. In a pure mechanical approach the IDR_{DS2} could be evaluated as the drift corresponding to the peak of the backbone according to Fardis' model (1997); the stiffness at this point can be computed according to the secant formulation according to Mainstone (1971). In this case too, the experimental basis for the evaluation of the IDR of the first storey was preferred and the value assumed is equal to 0.002 (Colangelo, 2012).
- DS3: *Large cracks in partition and infill walls, failure of individual infill panels.* At this stage the generic infill panel shows a significant strength drop with a consequent likely collapse of it. According to Fardis' backbone, the drift at this stage is strictly dependant on the softening stiffness of the infill. On the other hand the softening stiffness is characterized by a large variability depending on the specific kind of infill (mechanical properties, type of bricks,...). In such situation the experimental basis is the most reliable solution (Colangelo, 2012). Furthermore, it is worth to be noted that experimental data by Colangelo refer to the typical infills employed in residential buildings of the Mediterranean area. In this case the IDR_{DS3} is assumed equal to 0.012.

Once the characteristic IDR_{DS_i} are defined, the definition of S_{dDS_i} can be evaluated through a deformed shape defined *a priori*. In particular, the deformed shape at a given DS level is evaluated according the two following assumptions: (i) the IDR_{DS_i} is attained at the first storey; (ii) the deformed shape of the $n-1$ storeys is evaluated as function of their stiffness with that expected at the first storey.

In the case of DS1 and DS2 S_{dDS_i} is evaluated according to Equation (19). The IDR of the i th ($i > 1$) storey is computed considering an inverted triangular distribution of lateral forces as shown in Equation (20), in which H_i and H_j are the heights of the i^{th} and j^{th} storeys above the level of application of the seismic action (foundation or top of a rigid basement). The coefficient γ in Equation (19) is the average of the ratio, $\gamma_i = K_i / K_1$, between the stiffness of the i th storey (K_i) and that of the first storey (K_1), all evaluated considering the only infills' contribution and neglecting the concrete stiffness contribution at the different storeys.

$$S_{d|DS} = \frac{1}{\Gamma_1} (IDR_{DS} \cdot h_{1,int} + \gamma \cdot \sum_{i=2}^n IDR_i \cdot h_{int}) \quad (19)$$

$$IDR_i = IDR_{DS} \left(1 - \sum_{j=1}^{i-1} \frac{H_j}{\sum_{j=1}^n H_j} \right) \quad (20)$$

In the case of DS1 the stiffness of the all the storeys is still elastic; thus leading to $\gamma=1.0$. For DS2 a linear distribution of the stiffness along the height of the building is assumed. Thus, it is evaluated considering a secant stiffness at the first storey (Mainstone, 1971) and elastic at the top storey. Based on numerical and experimental results (e.g. Ricci 2011b; Colangelo, 2012), the secant stiffness was considered as the 25% of the elastic, leading to the evaluation of γ as shown in Equation (21).

$$\gamma = \frac{(K_{el} + K_{sec,Main})}{2K_{el}} = \frac{(K_{el} + 0.25K_{el})}{2K_{el}} = 0.625 \quad (21)$$

For DS3, $S_{d|DS3}$ is evaluated assuming the same deformed shape for the $n-1$ storeys as that computed for DS2 and the only displacement increasing is produced by IDR_{DS3} , as shown in Equation (22). The latter assumption implies that the unloading stiffness of the $n-1$ storeys is infinite.

$$S_{d|DS3} = S_{d|DS2} + \frac{(IDR_{DS3} - IDR_{DS2}) \cdot h_{int}}{\Gamma_1} \quad (22)$$

The definition of the $S_{d|DS_i}$ for the three DS allows the consequent definition of $S_a(T)_{|DS_i}$ through the IN2 curve. In fact, $S_{d|DS_i}$ is the expression of the characteristic equivalent SDOF displacement that represents the abscissa in the ADRS format in which the IN2 is computed. Thus, the IN2 curve becomes the tool by which $S_a(T)_{|DS_i}$ can be defined. Given $S_a(T)_{|DS_i}$, the switching to PGA_{DS_i} is pursued through a spectral scaling procedure. Each $S_a(T)_{|DS_i}$ is divided by the ratio of the spectral acceleration demand at $T_{1,inf}$ and the PGA demanded, $S_{a_d}(T_{1,inf})/PGA_d$.

Capacity curves and IN2 curves in terms of $S_{ea}(T_{eff})$ – obtained as explained above – are reported in Figure 13. Capacity curves parameters are also summarized in Table 7. Seismic capacity expressed in term of $S_{ae}(T_{eff})$ is reported for each DS and for each benchmark.

Finally, in Table 8, displacement capacities of the equivalent SDoF corresponding to the achievement of the analyzed DSs are reported.

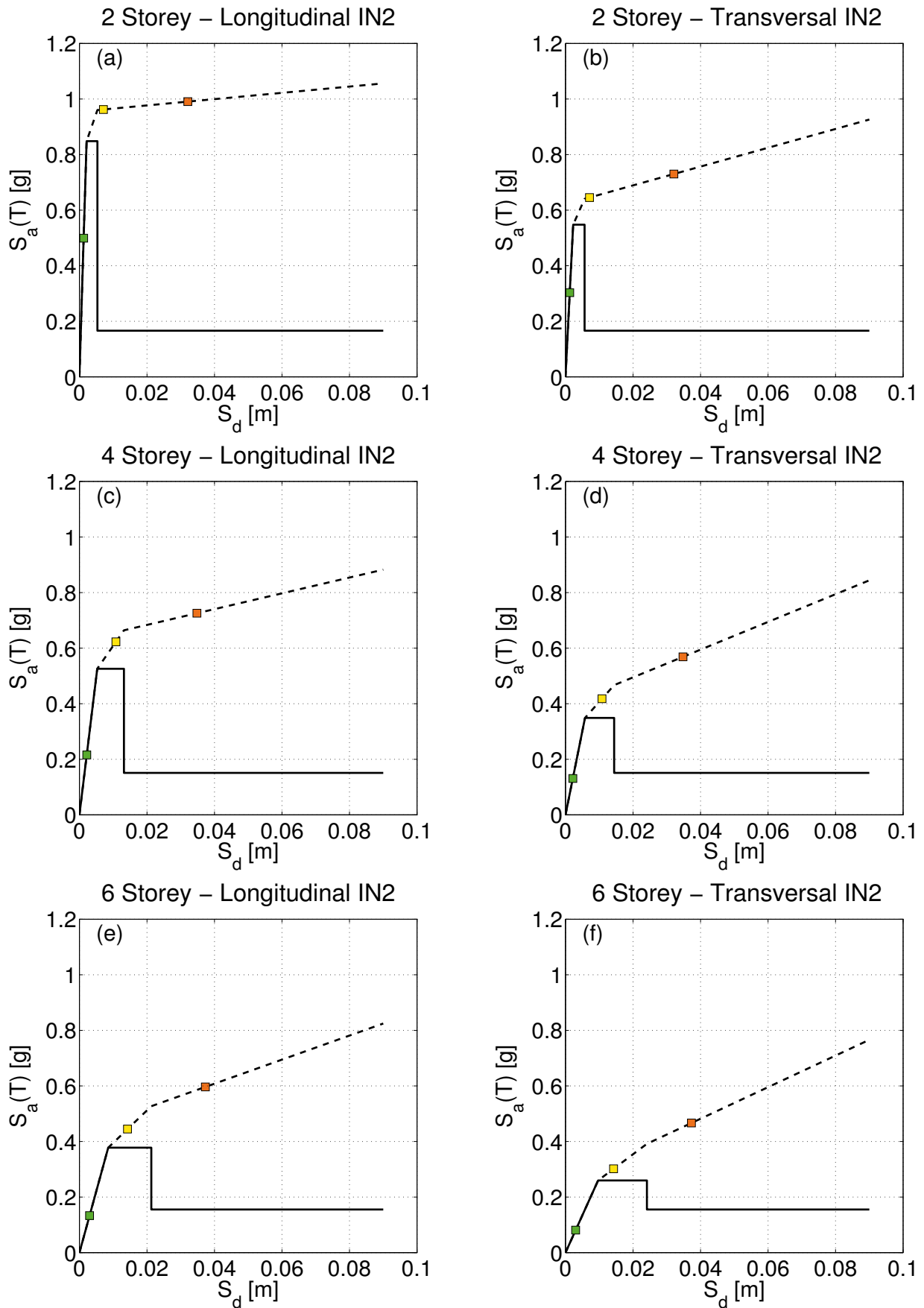


Figure 13. Multi-linearized capacity curves and IN2 curves in terms of $S_{ac}(T_{eff})$ – FAST approach

Table 7. Capacity curves parameters and $S_{ae}(T_{eff})$ capacity – FAST approach

Number of storeys	Direction	Capacity curve's parameters							$S_{ae}(T_{eff})$ capacity		
		T_{el}	T_{eff}	m_s	$C_{s,max}$	$C_{s,min}$	R_u	λ	DS1	DS2	DS3
		[s]	[s]		[g]	[g]			[g]	[g]	[g]
2	X	0.072	0.100	2.500	0.848	0.166	0.196	1.00	0.499	0.962	0.990
	Y	0.092	0.129	2.500	0.548	0.166	0.303	1.00	0.303	0.645	0.730
4	X	0.143	0.201	2.500	0.526	0.151	0.287	0.85	0.216	0.623	0.726
	Y	0.184	0.258	2.500	0.349	0.151	0.433	0.85	0.131	0.418	0.569
6	X	0.215	0.301	2.500	0.378	0.155	0.410	0.85	0.133	0.445	0.596
	Y	0.276	0.387	2.500	0.260	0.155	0.597	0.85	0.081	0.302	0.467

Table8. Displacement capacity of the equivalent SDoF – FAST approach

S_d Direction x	DS1	DS2	DS3	S_d Direction y	DS1	DS2	DS3
	[cm]	[cm]	[cm]		[cm]	[cm]	[cm]
2 storeys	0.13	0.71	3.21	2 storeys	0.125	0.708	3.208
4 storeys	0.22	1.08	3.48	4 storeys	0.216	1.080	3.480
6 storeys	0.30	1.42	3.73	6 storeys	0.300	1.423	3.731

7 COMPARATIVE DAMAGE ASSESSMENT

The results of the three different vulnerability approaches described allow a final comparison in terms of capacity curves and IN2 curves. On the other hand, notwithstanding the significance of the latter direct comparison, the final test-bed of each methodology is the evaluation of DS thresholds in terms of spectral displacements and PGA.

Figure 14 compare the capacity curves and the IN2 curves in terms of $S_a(T_{eff})$, while Figure 14 provides a similar comparison in terms of PGA. The scaling procedure of the IN2 ordinate is made according the same criterion for the three methods. In fact, the ratio between the spectral acceleration at T_{eff} and the PGA on rigid soil type of the spectrum considered represents the scaling factor that resizes the ordinates of the IN2 curves; thus, it allows switching from $S_a(T_{eff})$ to PGA. In Figure 14 and 15 the threshold of the three DS considered are also shown for the three vulnerability methods.

In Table 9, damage threshold in terms of PGA on rigid soil (A soil class) are shown for the three methodologies considered. Given the fact that the constant shape spectra of Eurocode 8 is characterized by a fixed soil amplification factor S ; equal to 1.2, 1.15, 1.35, and 1.4, respectively for soil types B to E; the PGA values in Table 9 can be easily scaled aimed at accounting for the effect of soil amplification on damage thresholds.

Table 9. Comparison between PGA capacities

Number of storeys	Direction	PGA DAMAGE STATE								
		EXACT			POST			FAST		
		DS1	DS2	DS3	DS1	DS2	DS3	DS1	DS2	DS3
		[g]	[g]	[g]	[g]	[g]	[g]	[g]	[g]	[g]
2	X	0.226	0.427	0.459	0.254	0.420	0.447	0.211	0.407	0.419
	Y	0.115	0.235	0.287	0.140	0.245	0.295	0.114	0.243	0.275
4	X	0.083	0.199	0.250	0.106	0.196	0.236	0.064	0.185	0.215
	Y	0.046	0.122	0.161	0.064	0.131	0.191	0.039	0.124	0.168
6	X	0.052	0.137	0.205	0.073	0.150	0.186	0.039	0.132	0.177
	Y	0.032	0.083	0.114	0.047	0.105	0.155	0.024	0.089	0.138

Relative errors between the three vulnerability methodologies are shown in Table 10 and 11, respectively for damage thresholds in terms of PGA and spectral displacements. Relative errors of *EXACT* with respect to *POST* approach are shown on the right, while, on the left, the relative errors of *FAST* with respect to *POST* are shown.

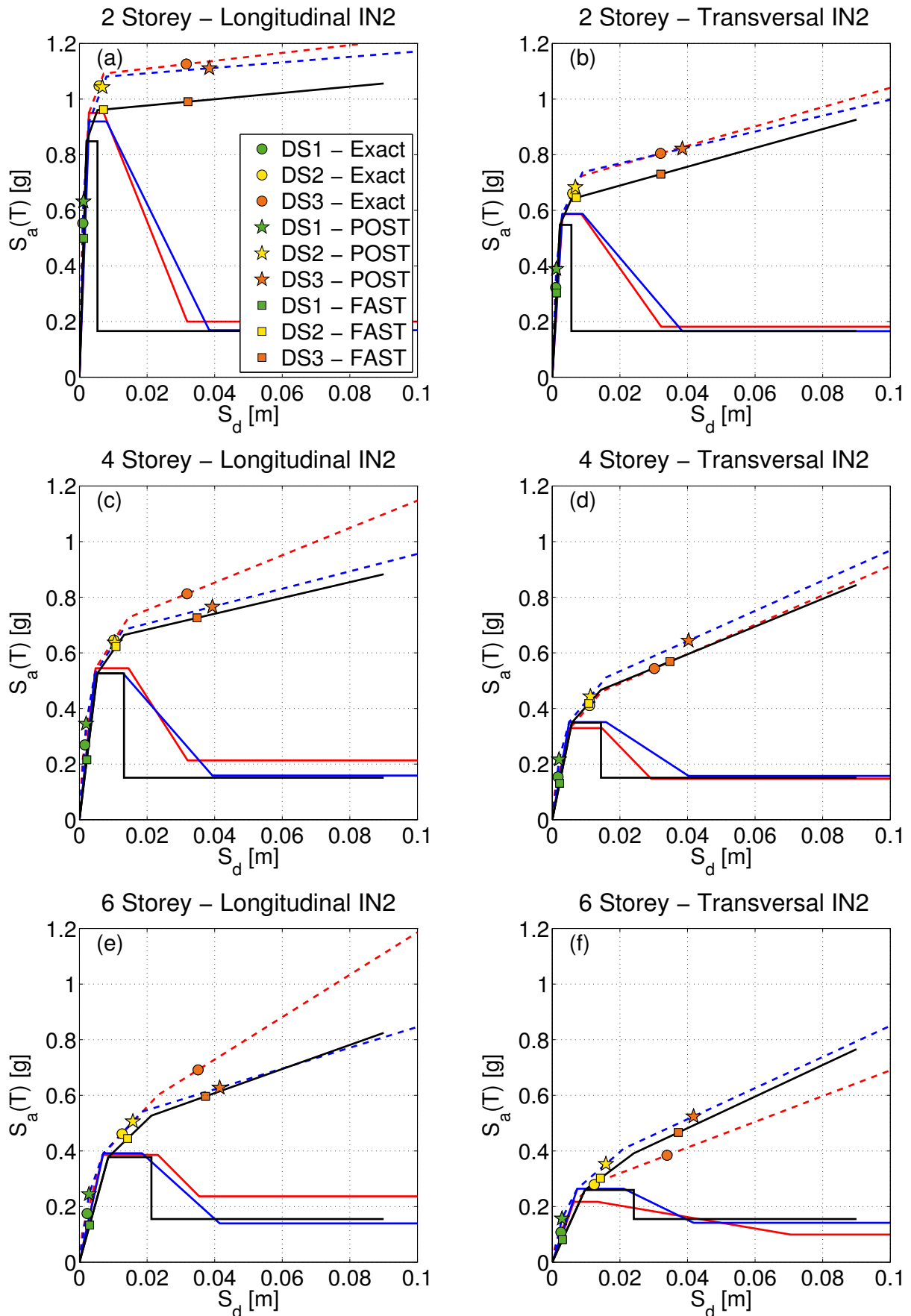


Figure 14. Comparison between IN2 curves in terms of S_a for EXACT (red), POST (blue) and FAST (black) approaches.

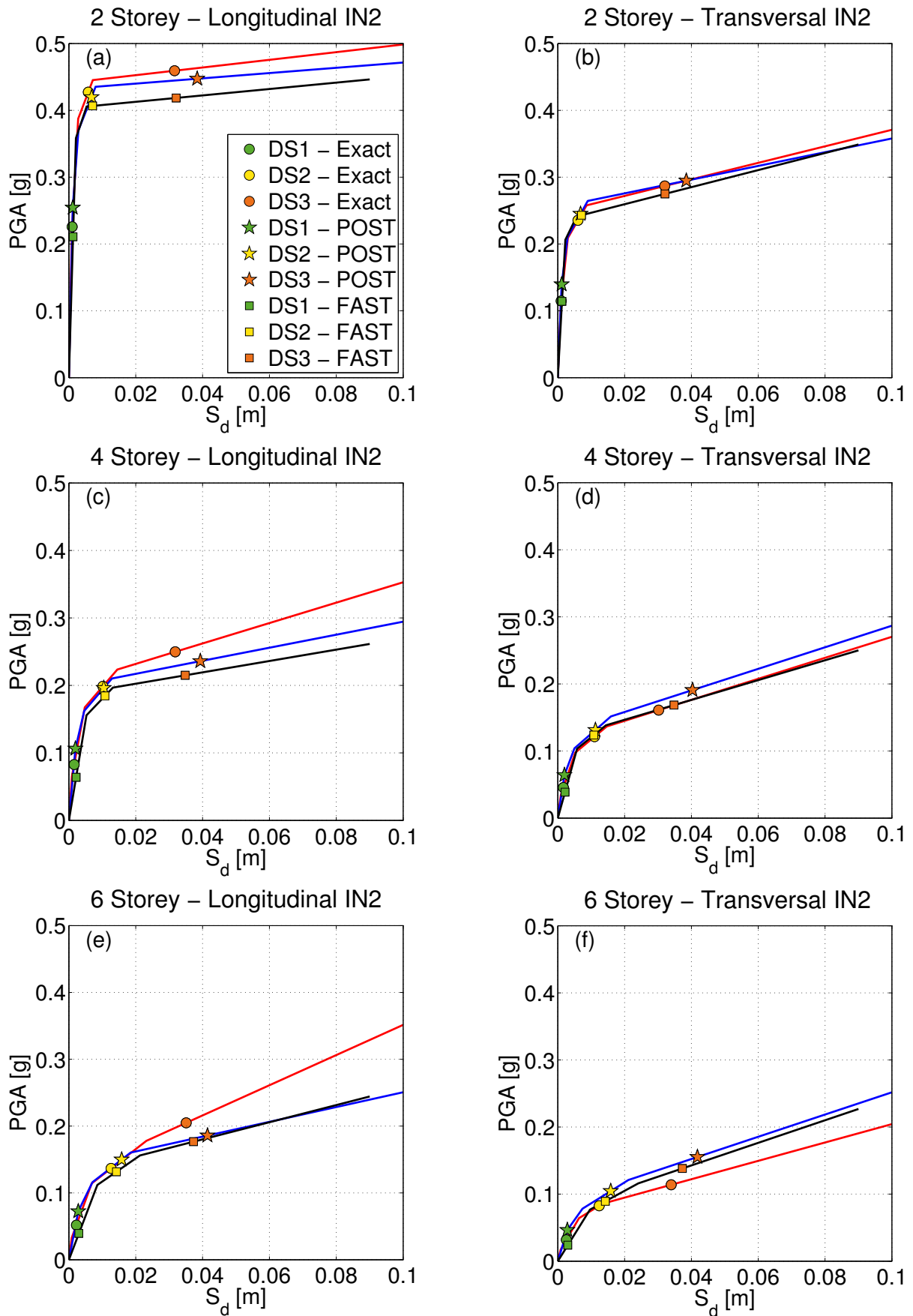


Figure 15 Comparison between IN2 curves in terms of PGA for *EXACT* (red), *POST* (blue) and *FAST* (black) approaches.

Table 10. Errors referred to PGA capacity

Number of storeys	Direction	$e^{PGA} \frac{EXACT-POST}{POST}$			$e^{PGA} \frac{FAST-POST}{POST}$		
		DS1	DS2	DS3	DS1	DS2	DS3
2	X	-0.112	0.018	0.027	-0.171	-0.032	-0.064
	Y	-0.177	-0.040	-0.027	-0.182	-0.008	-0.067
4	X	-0.222	0.012	0.059	-0.399	-0.060	-0.089
	Y	-0.289	-0.075	-0.156	-0.395	-0.058	-0.117
6	X	-0.284	-0.089	0.103	-0.456	-0.122	-0.049
	Y	-0.314	-0.210	-0.267	-0.485	-0.146	-0.110

Table 11. Errors referred to displacement capacity of the equivalent SDoF

Number of storeys	Direction	$e^{Sd/DS_i} \frac{EXACT-POST}{POST}$			$e^{Sd/DS_i} \frac{FAST-POST}{POST}$		
		DS1	DS2	DS3	DS1	DS2	DS3
2	X	-0.166	-0.144	-0.177	0.064	0.044	-0.165
	Y	-0.141	-0.113	-0.168	0.063	0.040	-0.166
4	X	-0.194	-0.027	-0.191	0.102	0.033	-0.115
	Y	-0.152	-0.024	-0.018	0.090	-0.042	-0.137
6	X	-0.200	-0.202	-0.154	0.067	-0.099	-0.101
	Y	-0.102	-0.218	-0.188	0.043	-0.102	-0.107

The observation of the IN2 curves in terms of $S_a(T_{eff})$ in [Figure 14](#) shows how the *FAST* approach is always conservative respect to both *POST* and *EXACT* approach. The explanation of the latter observation can be found in the differences between the curves that, in turn, correspond to the different hypotheses of each methodology:

- Elastic and effective periods evaluated according each methodology are similar to each other.
- The three approaches, excluding the two storey case, have similar values of $C_{s,max}$, which is mostly defined by infill contribution. It confirms the reliability of [Equation \(16\)](#) in which α was considered equal to 0.5. In the case of two storeys building the approximate evaluation of α is evidently underestimated.
- The value of ductility μ_s evaluated in the *EXACT* and *POST* approaches is generally higher with respect to the value (equal to 2.5) assumed in the case of *FAST* approach. The latter result leads to a lower slope of the second branch of the IN2 curve according to *FAST* method, as it can be seen in [Figure 14](#).

- The simplified simulated design procedure adopted in the *FAST* approach seems to lead to a value of $C_{s,min}$ generally lower with respect to the more accurate simulated design approaches in the *POST* and *EXACT*. Such results, given the R- μ -T relationship employed leads to lower slope of the third branch of the IN2 curve.
- The highest relative errors between large scale methodologies, *POST* and *FAST*, versus the detailed *EXACT* approach are observed in the case of the six storey building. The latter is the result of single storey plastic mechanism made in both the large scale approaches. In particular, according to the detailed assessment in the *EXACT* approach the plastic mechanism involves more than one storey; thus, in the longitudinal direction a highest value of $C_{s,min}$ and a lower value of $C_{s,max}$ can be observed in *EXACT* results.

Differences in the IN2 curves plotted in terms of $S_a(T)$ are not affected by the homothetic scaling procedure that leads to the IN2 curves in terms of PGA on rigid soil (see [Figure 15](#)).

Furthermore, in [Table 10](#) the comparison between the three methods is provided in terms of characteristic displacements of the three damage states considered. It is worth to note that the general trends of the relative errors are acceptable. It is interesting to observe that the *POST* approach leads, respect to the *EXACT* approach DS displacements always higher, notwithstanding the shear-type hypothesis adopted in the first method that would conceptually lead to lower displacements. The latter result can be explained by the different value of the first mode participant factors (Γ_1) considered in the two methods, lower in the case of the *POST* approach. Conversely, the *FAST* approach leads to higher displacement values with respect to the *POST* in the case of DS1, while to lower displacements with respect to the *POST* in the case of DS3 for the all three benchmark structures considered.

The results of the three approaches described in this study can be finally summarized by the comparisons in terms of PGA capacities at the three different DS considered, as shown in [Table 11](#). The relative errors can be considered acceptable. The *POST* is generally non conservative with respect to the *EXACT* results, especially if the DS1 is considered. The *FAST* approach is always conservative with respect to the *POST*. It is worth to note that the significant differences in terms of PGA for DS1 are clearly a result of the procedure to increase the accuracy in the elastic branch of the IN2 curve employed in the case of the *EXACT* and *POST* approach. Such increase in the accuracy was not employed in the *FAST* approach given its intrinsically approximate nature that does not fit with the more accurate procedure suggested in Dolsek and Fajfar (2005).

It should be emphasized how the approximate procedure in general, and in particular the *FAST* method, lead to results that are comparable to the results of the *EXACT* detailed approach;

especially if the poor quality of the information and low computational efforts required are considered.

Finally, the results obtained through the three vulnerability approaches in terms of PGA are compared with the shake map of the 20th of May mainshock according to INGV (see [Figure 16](#)). First of all it should be highlighted that the damage thresholds in terms of PGA shown in [Table 9](#) are computed for the case of rigid soil (A soil class) and for the constant shape spectra according to EC8 (type 1). Conversely, even if on the basis of very macroscopic geological scale, the most of the area struck by the earthquake is characterized by D soil class. The latter aspect is accounted for considering the D soil amplification factor according to EC8 (equal to 1.35).

By means of a simple amplification of the PGA values in [Table 9](#), PGA thresholds at each damage state can be estimated for the case of D soil class. In [Table 12](#), for each vulnerability methodology and each DS, the minimum PGA among the two principal directions of the benchmark buildings are shown.

The analysis of the data provided by ISTAT (see section 2), aimed at characterizing the building stock, showed that the area struck by the earthquake was mostly characterized by low to medium rise buildings (from 2 up to 4 storeys). Hence, the comparisons with the PGA data are referred to the first two benchmark buildings.

From [Table 12](#) the following information can be extrapolated, considering the mean value obtained from the three methodologies:

- DS1 is equal to 0.17g for the 2 storey buildings, while to 0.07g for the 4 storey building
- DS2 is equal to 0.33g for the 2 storey buildings, while to 0.17g for the 4 storey building
- DS3 is equal to 0.38g for the 2 storey buildings, while to 0.24g for the 4 storey building

The comparison of the numerical PGA thresholds, at the three DSs, and the shake map allows some preliminary remarks. In particular, such remarks are affected by two basic hypotheses: (i) a uniform distribution of the RC buildings on the area is assumed, given the lack of disaggregated data from the ISTAT reference; (ii) the benchmark buildings considered are defined as representative of the whole building stock.

First of all, it is easy to recognize that numerical results predict a DS3 damage only in the case of RC buildings localized in the epicentral area. Furthermore, higher buildings are on average susceptible of more significant damage given the PGA of the earthquake. According to the numerical data, most of four storeys buildings should be characterized by DS1 and DS2 (with the exception of the only epicentral area).

Even if the fact that RC buildings are not so frequent in the area, numerical results show a fair to good agreement with the data collected during in-field campaigns after the earthquake (e.g., [Decanini et al., 2012](#), [EPICentre Field Observation Report No. EPI-FO-290512, 2012](#)), and visually classified according to EMS-98, as shown in the examples in [Figure 5](#).

Table 12. Minimum PGA capacities

Number of storeys	PGA DAMAGE STATE								
	EXACT			POST			FAST		
	DS1	DS2	DS3	DS1	DS2	DS3	DS1	DS2	DS3
	[g]	[g]	[g]	[g]	[g]	[g]	[g]	[g]	[g]
2	0.16	0.32	0.39	0.19	0.33	0.40	0.15	0.33	0.37
4	0.06	0.16	0.22	0.09	0.18	0.26	0.05	0.17	0.23
6	0.04	0.11	0.15	0.06	0.14	0.21	0.03	0.12	0.19

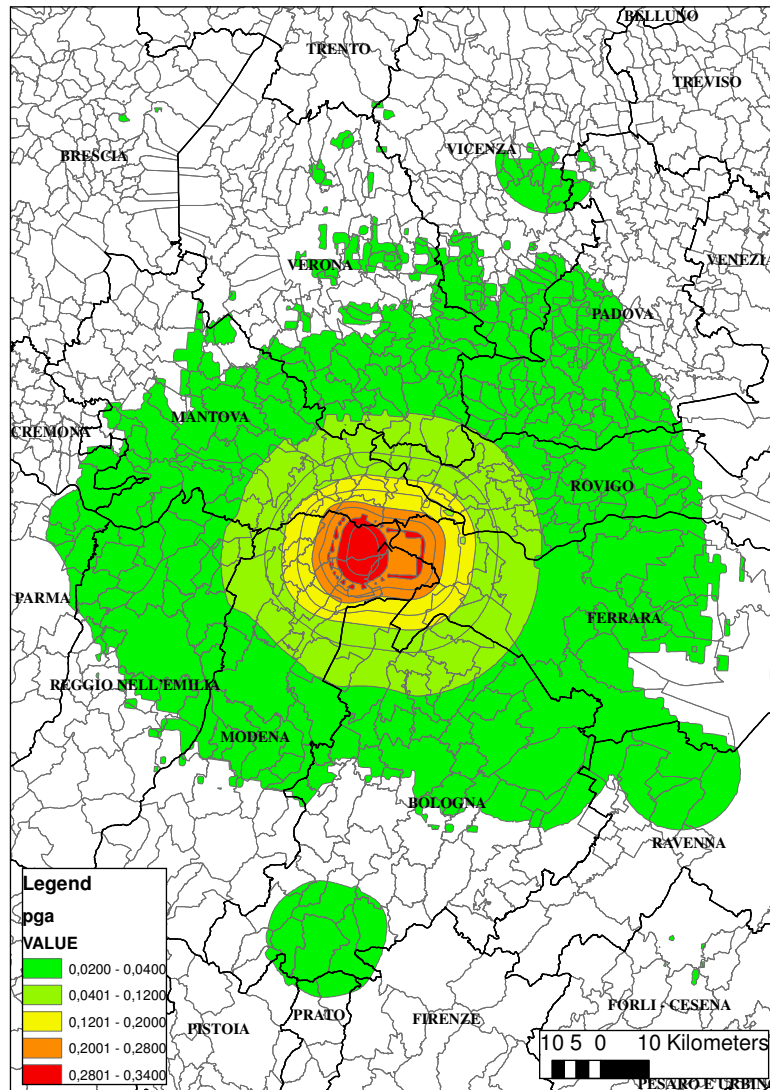


Figure 16. PGA shake map of the 20th of May event according to INGV.

8 CONCLUSIONS AND PERSPECTIVES

A three level vulnerability approach for the evaluation of the performances of RC infilled structures was provided and aimed at looking into the observed performances of RC structures during the 2012 Emilia earthquake. The vulnerability study was pursued on three benchmark buildings representative of the building stock of the area struck by the earthquake. The historical and recent evolution of seismic codes and the seismic classification of the area were considered to assess the design approach that the benchmark structures considered should have to be representative of the most common construction practice at the site.

The three damage assessments were pursued on the benchmark structures beginning with a detailed push-over based methodology, named EXACT. Two large scale vulnerability methodologies were described and compared in terms of basic hypotheses. The only first three grades of damage according to EMS-98 scale were considered; since for those three grades a mechanical and empirical evaluation of the displacement capacities can be carried out on the basis of the behavior of masonry infills.

Results in terms of spectral displacements, spectral acceleration and PGA characterizing the three damage states, according to the three methodologies were compared. The two large scale approaches showed a fair to good agreement with the results of the detailed assessment. Relative errors are characterized by a conservative general trend that in some way can provide a validation of the large scale methodologies provided.

Finally a comparison with the registered PGA during the mainshock event of the 2012 Emilia sequence explains the limited damage observed to RC structures in the area struck by the earthquake. In fact, in the only epicentral zone, the PGA characterizing moderate structural damage and vey heavy nonstructural damage (grade 3 according to EMS-98) was exceeded. The study provided shows the reliability of the large scale approaches also in terms of observed damage.

American Society of Civil Engineers (ASCE), Seismic Rehabilitation of Existing Buildings, ASCE/SEI 41-06, Reston, Virginia, 2007.

Augenti N., (2009). Un database per l'archiviazione e l'analisi di dati sperimentali relativi alle murature. Proceedings of the 3rd conference Wondermasonry - Workshop on design and rehabilitation of masonry structures, 8 October, Lacco Ameno, Italy.

Bal I.E., Crowley H., Pinho R., Gulay F.G., 2007. Structural characteristics of Turkish RC building stock in Northern Marmara region for loss assessment applications. ROSE Research Report No. 2007/03, IUSS Press, Pavia, Italy.

Benavent-Climent A., Akiyama H., Lopez-Almansa F., Pujades L.G. (2004). Prediction of ultimate earthquake resistance of gravity-load designed RC buildings. Engineering Structures 26, 1103-1113.

- Bindi D, Pacor F, Luzi L, Puglia R, Massa M, Ameri G, Paolucci R, (2011). Ground motion prediction equations derived from the Italian strong motion database, *Bulletin of Earthquake Engineering*, 9(6), 1899-1920.
- Biskinis D. and Fardis M. N. (2010a), Deformations at flexural yielding of members with continuous or lap-spliced bars. *Structural Concrete* 11(3): 128-138.
- Biskinis DE and Fardis MN (2010b) Flexure-controlled ultimate deformations of members with continuous or lap-spliced bars. *Structural Concrete* 11(2): 93-108.
- Borzi B., Elnashai A. (2000). Refined force reduction factor for seismic design. *Engineering Structures* 22, 1244-1260.
- CEN (2004) Eurocode 8: design of structures for earthquake resistance—Part 1: general rules, seismic actions and rules for buildings. European Standard EN 1998-1:2003- Comité Européen de Normaliation, Brussels.
- Celarec, D., Ricci, P., Dolšek, M. (2012). The sensitivity of seismic response parameters to the uncertain modelling variables of masonry-infilled reinforced concrete frames. *Engineering Structures*, 35, 165-177.
- Chioccarelli E, De Luca F, Iervolino I. (2012a), Preliminary study of Emilia (May 20th 2012) earthquake ground motion records V2.11, [available at <http://www.reluis.it>].
- Chioccarelli, E., F. De Luca and I. Iervolino (2012b). Preliminary study of Emilia (May 29th 2012) earthquake ground motion records V1.0, [available at <http://www.reluis.it>].
- Chopra A.K., Chintanapakdee C., (2004). Inelastic Deformation Ratios for Design and Evaluation of Structures: Single-Degree-of-Freedom Bilinear Systems. *ASCE Journal of Structural Engineering*, 130(9), 1309-1319.
- Colangelo F. (2012). A simple model to include fuzziness in the seismic fragility curve and relevant effect compared with randomness. *Earthquake Engineering and Structural Dynamics*, 41, 969-986.
- Cosenza E., Manfredi G., Polese M., Verderame G.M., (2005). A multilevel approach to the capacity assessment of existing RC buildings. *Journal of Earthquake Engineering*, 9(1), 1-22.
- CS.LL.PP.; 2009: Istruzioni per l'applicazione delle norme tecniche delle costruzioni. *Gazzetta Ufficiale della Repubblica Italiana*, 47.
- Decanini L., Liberatore D., Liberatore L., Sorrentino L., (2012). PRELIMINARY REPORT ON THE 2012, MAY 20TH, EMILIA EARTHQUAKE v1.0, [available at http://www.eqclearinghouse.org/2012-05-20-italy-it/files/2012/06/Emilia2012_DecaniniLiberatoreLiberatoreSorrentino_v1.pdf].
- Decreto Ministeriale del 16/1/1996 (1996) Norme tecniche per le costruzioni in zone sismiche. *Gazzetta Ufficiale della Repubblica Italiana*, 29 del 5/2/1996 (in Italian)
- Decreto Ministeriale del 14 Gennaio 2008: Norme tecniche per le costruzioni. *Gazzetta Ufficiale della Repubblica Italiana*, 29. 4/2/2008 (in Italian).
- Decreto Ministeriale n. 40 del 3/3/1975 (1975) Approvazione delle norme tecniche per le costruzioni in zone sismiche. *Gazzetta Ufficiale della Repubblica Italiana*, 93 dell'8/4/1975 (in Italian)
- De Luca F., 2011. Records, capacity curve fits and reinforced concrete damage states within a performance based earthquake engineering framework. PhD thesis. Department of Structural Engineering, University of Naples Federico II. Advisors: G. Manfredi, I. Iervolino, G.M. Verderame. Available at <http://wpape.unina.it/flavia.deluca/>.

- De Luca F., Verderame G.M., Gomez-Martinez F., Perez-Garcia A., (2012). The structural role played by masonry infills on RC building performances after the 2011 Lorca, Spain, earthquake. *Bulletin of Earthquake Engineering*, (under review).
- De Marco R., Marsan P. (Eds.), (1986). *Atlante della classificazione sismica del territorio nazionale*, Servizio Sismico del Consiglio Superiore dei Lavori Pubblici, Istituto Poligrafico e Zecca dello Stato Italiano, Roma.
- Dolce M., Cardone D., Ponzo F.C., Valente C., (2005). Shaking table tests on reinforced concrete frames without and with passive control systems. *Earthquake Engineering and Structural Dynamics*, 34, 1687-1717.
- Dolšek, M., Fajfar, P. (2004a). Inelastic spectra for infilled reinforced concrete frames. *Earthquake Engineering and Structural Dynamics*, 33(15), 1395-1416.
- Dolšek, M., Fajfar, P. (2004b). IN2 - A simple alternative for IDA. *Proceedings of the 13th World Conference on Earthquake Engineering*, Vancouver, B.C., Canada, August 1-6. Paper No. 3353.
- Dolšek, M., Fajfar, P. (2005). Simplified non-linear seismic analysis of infilled reinforced concrete frames. *Earthquake Engineering and Structural Dynamics*, 34(1), 49-66.
- Dolšek, M., Fajfar, P. (2008). The effect of masonry infills on the seismic response of a four-storey reinforced concrete frame – a deterministic assessment. *Engineering Structures*, 30(7), 1991-2001.
- EPICentre Field Observation Report No. EPI-FO-200512 (2012), The 20th May 2012 EmiliaRomagna Earthquake, [available at http://www.ucl.ac.uk/~ucestor/research-earthquake/EPICentre_Report_EPI-FO-200512-v2.pdf].
- EPICentre Field Observation Report No. EPI-FO-290512 (2012), The 29th May 2012 EmiliaRomagna Earthquake, [available at http://www.ucl.ac.uk/~ucestor/research-earthquake/EPICentre_Report_EPI-FO-290512.pdf].
- Fardis, M.N. (2007). LESSLOSS – Risk mitigation for earthquakes and landslides. Guidelines for displacement based design of buildings and bridges. Report No. 5/2007, IUSS Press, Pavia, Italy.
- Galasso C., Cosenza E., Maddaloni G. (2011). Statistical analysis of reinforcing steel properties for seismic design of RC structures. *Proceedings of the 14th European Conference on Earthquake Engineering*, August 30-September 3, Ohrid, Republic of Macedonia.
- Giovinazzi S., 2005. The vulnerability assessment and the damage scenario in seismic risk analysis. PhD Thesis, Technical University Carolo-Wilhelmina at Braunschweig, Braunschweig, Germany and University of Florence, Florence, Italy.
- Giovinazzi S., Lagomarsino S., (2004). A macroseismic method for the vulnerability assessment of buildings. *Proceedings of the 13th World Conference on Earthquake Engineering*, Vancouver, Canada, August 1-6. Paper No. 896.
- Gomez-Martinez F., Perez-Garcia A., De Luca F., Verderame G.M., Manfredi G., (2012). Preliminary study of the structural role played by masonry infills on RC building performances after the 2011 Lorca, Spain, earthquake, *Proceedings of the 15th World Conference on Earthquake Engineering*, September 24-28, Lisbon, Portugal.
- Goretti A. and Di Pasquale G., (2006). Technical emergency management. In: Oliveira C.S., Roca A., and Goula X. Editors; *Assessing and managing earthquake risk*, Springer, chapter 16.

- Iervolino, I. (2012). Probabilità e salti mortali: le insidie della validazione dell'analisi di pericolosità attraverso l'occorrenza di singoli terremoti. *Progettazione Sismica*. IUSS Press, Pavia, Italy. (in Italian, in press).
- Iervolino I., Manfredi G., Polese M., Verderame G.M., Fabbrocino G., (2007). Seismic risk of R.C. building classes. *Engineering Structures*, 29(5), 813-820.
- Iervolino I., De Luca F., Chioccarelli E., (2012). Peak and cyclic, elastic and inelastic, engineering seismic demand in the 2012 Emilia sequence: preliminary analysis, *Annals of Geophysics*, (under review).
- Lai C, Foti S, Rota M, (2009). *Input sismico e stabilità geotecnica dei siti in costruzione*. IUSS Press, Pavia, Italy.
- Mainstone R.J., 1971. On the stiffnesses and strengths of infilled frames. *Proceedings of the Institution of Civil Engineering*, Supplement IV, 57-90.
- Manfredi G., Ricci P., Verderame G.M. (2012), Influence of Infill Panels and Their Distribution on Seismic Behavior of Existing Reinforced Concrete Buildings, *The Open Construction and Building Technology Journal*, 2012, 6, (Suppl 1-M1).
- McKenna, F., Fenves, G.L., Scott, M.H. (2004). *OpenSees: Open System for Earthquake Engineering Simulation*. Pacific Earthquake Engineering Research Center. University of California, Berkeley, CA, USA. <http://opensees.berkeley.edu>.
- Ordinanza del Presidente del Consiglio dei Ministri n. 3274 del 20/3/2003 (2003) Primi elementi in materia di criteri generali per la classificazione sismica del territorio nazionale e di normative tecniche per le costruzioni in zona sismica. G.U. n. 105 dell'8/5/2003 (in Italian).
- Panagiotakos, T.B., Fardis, M.N. (1996). Seismic response of infilled RC frames structures. 11th WorldConference on Earthquake Engineering, Acapulco, México, June 23-28. Paper No. 225.
- Pecce M, Polese M, Verderame GM. Seismic vulnerability aspects of RC buildings in Benevento. In: Pecce M, Manfredi G, Zollo A. editors. *The many facets of seismic risk CRdC AMRA*; 2004.
- Regio Decreto Legge n. 2229 del 16/11/1939. Norme per la esecuzione delle opere in conglomerate cementizio semplice od armato. G.U. n. 92 del 18/04/1940. (in Italian).
- Ricci, P. (2010). Seismic vulnerability of existing RC buildings. Ph.D. Thesis. University of Naples Federico II, Naples, Italy.
- Ricci, P., De Luca, F., Verderame, G.M. (2011a). 6th April 2009 L'Aquila earthquake, Italy – Reinforced concrete building performance. *Bulletin of Earthquake Engineering* 9(1),285-305.
- Ricci, P., Verderame G.M., Manfredi G., (2011b) Analytical investigation of elastic period of infilled RC MRF buildings, *Engineering Structures* 33(2), 308-319.
- Ricci P., De Risi M.T., Verderame G.M., Manfredi G., (2012). Influence of infill distribution and design typology on seismic performance of low- and mid-rise RC building. *Bulletin of Earthquake Engineering*, (under review).
- Rossetto T., Elnashai A., (2005). A new analytical procedure for the derivation of displacement-based vulnerability curves for populations of RC structures. *Engineering Structures*, 7(3), 397-409.
- STIL, software, (2012) Verderame G.M., Ricci P., Esposito E., Manfredi G. Available at www.reluis.it.

- Stucchi M, Meletti C, Montaldo V, Crowley H, Calvi GM, Boschi E. Seismic Hazard Assessment (2003-2009) for the Italian Building Code, *Bulletin of the Seismological Society of America* 2011; 101(4):1885-1911.
- Verderame GM, Stella A., Cosenza E., (2001). Le proprietà meccaniche degli acciai impiegati nelle strutture in c.a. realizzate negli anni 60'. X Convegno nazionale "L'Ingegneria Sismica in Italia", Potenza-Matera, 9-13 September.
- Verderame G.M., Polese M., Mariniello C., Manfredi G., (2010a). A simulated design procedure for the assessment of seismic capacity of existing reinforced concrete buildings, *Advances in Engineering Software*, 41, 323–335.
- Verderame, G.M., Ricci, P., Manfredi, G., Cosenza, E. (2010b). Ultimate chord rotation of RC columns with smooth bars: some considerations about EC8 prescriptions. *Bulletin of Earthquake Engineering*, 8(6),1351-1373.